Copyright Warning & Restrictions

The copyright law of the United States (Title 17, United States Code) governs the making of photocopies or other reproductions of copyrighted material.

Under certain conditions specified in the law, libraries and archives are authorized to furnish a photocopy or other reproduction. One of these specified conditions is that the photocopy or reproduction is not to be "used for any purpose other than private study, scholarship, or research." If a, user makes a request for, or later uses, a photocopy or reproduction for purposes in excess of "fair use" that user may be liable for copyright infringement,

This institution reserves the right to refuse to accept a copying order if, in its judgment, fulfillment of the order would involve violation of copyright law.

Please Note: The author retains the copyright while the New Jersey Institute of Technology reserves the right to distribute this thesis or dissertation

Printing note: If you do not wish to print this page, then select "Pages from: first page # to: last page #" on the print dialog screen

ABSTRACT

EMISSIVITY MEASUREMENTS AND MODELING OF SILICON RELATED MATERIALS

by
Vijay Krishnamurthy

The objective of the thesis was to study the radiative properties of silicon related materials for applications in rapid thermal proceesing. In particular, three distinct materials have been considered – Silicon, SIMOX and Tantalum.

The research highlights are :Establishment of spectral emissometry as a novel, reliable and reproducible technique for a) Determination of wavelength and temperature dependent reflectivity, transmissivity, emissivity of silicon related materials and structures. The emissometer operates in the wavelength range of 1-20μm and temperature range of 300-1200K. b) Establishment of methodoligies to obtain the fundemental constants. Effects of wavelength, temperature, total available free carriers by doping types have been considered. Comparisons have been sought with the available knowledge of "α" in the litreture by the extensive use of the Multi-Rad model. This is a state of the art model that has been developed by MIT/SEMATECH.

EMISSIVITY MEASUREMENTS AND MODELING OF SILICON RELATED MATERIALS

by
Vijay Krishnamurthy

A Thesis
Submitted to the Faculty of
New Jersey Institute of Technology
In Partial Fulfillment of the Requirements for the degree of
Master of Science in Electrical Engineering

Department of Electrical and Computer Engineering

August 1999

APPROVAL PAGE

Emissivity Measurements and Modelling of Silicon related materials

Vijay S. Krishnamurthy

Dr. N.M. Ravindra, Thesis Advisor
Professor, Dept. of Physics, NJIT

Dr. Kenneth Sohn, Committee Member
Associate Chair, Dept. of Electrical and Computer Engineering, NJIT

Dr. Edwin Hou, Committee Member
Associate Director of Computer Engineering Programs, NJIT

BIOGRAPHICAL SKETCH

Author : Vijay Krishnamurthy

Degree : Master of Science in Electrical Engineering

Date : August 1999

Undergraduate and Graduate Education :

- Master of Science in Electrical Engineering,
  New Jersey Institute of Technology, Newark, NJ,1999

- Bachelor of Science in Electrical Engineering,
  RVCE, Bangalore, India, 1997

Major : Electrical Engineering

To my beloved family and friends

ACKNOWLEDGEMENT

I would like to express my deep appreciation to Dr. N.M. Ravindra, for support and encouragement. Special thanks to Dr. K. Sohn, E. Hou for actively participating in my committee. I would also like to thank my friends who helped me during the thesis.

TABLE OF CONTENTS

TABLE OF CONTENTS
(Continued)

CHAPTER 1

INTRODUCTION

Silicon technology has remained as the dominant force in integrated circuit fabrication and is likely to retain this position for the forseeable future. The current trend in silicon device manufacturing has been to increase physical dimensions of silicon wafers and reduce device size [1]. This has led to some novel processes such as Rapid Thermal Processing (RTP), Rapid Thermal Chemical Vapor Deposition (RTCVD) [2] and Metal Organic Molecular Beam Epitaxy (MOMBE).

In semiconductor manufacturing processes, the precise temperature of the wafer surface is the most important parameter. Any change in the wafer's temperature means a change in the annealing temperature or thickness and/or uniformity of the grown or deposited film/s. The major temperature monitoring techniques utilized in semiconductor manufacturing are thermocouples and pyrometers.

The objective of this research is to study the radiative properties of silicon and silicon related materials and structures for temperature determination. To achieve this objective, a novel spectral emissometer has been utilized to yield the emissivity, reflectivity and transmissivity as function of wavelength and temperature in the range of 1-20μm and 300-1200K, respectively. The spectral emissometer has been utilized extensively to measure the radiative properties of (a) single versus double side polished silicon wafers, (b) silicon as a function of doping, (c) SiO_2/Si, with various oxide thicknesses (d) SIMOX (Si/SiO_2/Si) and (e) Tantalum .

In Chapter 2, the background of semiconductors and their properties, particularly silicon, are discussed. In Chapter 3, the fundamentals of radiative properties are discussed with their relationship to optical and electrical properties. The fundamentals of emissivity and radiative properties are presented in Chapter 4. Spectral emissometer is established as the tool for emissivity and measurements of related optical properties are discussed in Chapter 5. In Chapter 6, the discussion of the experimental results are presented. In addition, simulation results, based on a model – Multi-rad developed by MIT/ SEMATECH, are presented. The emissivity values for selected wavelengths are tabulated in this chapter. Conclusions and remarks based on these studies are presented in the last chapter.

CHAPTER 2

BACKGROUND

2.1 Fundamentals

2.1.1 Semiconductor Materials

Over the years, many semiconductors have been investigated. Semiconductor materials are found in column IV and the neighboring columns of the periodic table as shown in the Fig. 2.1.

The column IV semiconductors, silicon and germanium, are elemental semiconductors. In addition to the elemental materials, compounds of column III and column V atoms, as well as certain combinations from II and VI, make up the intermetallic, or compound semiconductors. In addition, there are numerous semiconductor materials. The wide variety of electronic and optical properties of these semiconductors provide the device engineer with great flexibility in the design and fabrication of electronic and optoelectronic devices. The elemental semiconductor Ge was widely used in the early days of semiconductor development for the fabrication of transistors and diodes.

Silicon is now used for majority of rectifiers, transistors and integrated circuits. However, the III-V compounds are widely used in high-speed devices requiring the emission or absorption of light. III-V compounds such as GaAs and GaP are commonly utilized in the fabrication of light emitting diodes (LEDs). Ternary compounds such as GaAsP and quadrinary compounds such as InGaAsP can be grown to provide added flexibility in choosing material properties. Fluorescent materials such as those used in

Period	column II	III	IV	V	VI
2		B Boron	C carbon	N Nitrogen	
3	Mg Magnesium	Al Aluminum	Si Silicon	P Phosphorus	S sulfur
4	Zn Zinc	Ga Gallium	Ge Germainum	As Arsenic	Se Selenium
5	Cd Cadmium	In Indium	Sn Tin	Sb Antimony	Te Tellurium
6	Hg Mercury		Pb Lead		

Fig. 2.1 Portion of the periodic table related to Semiconductors [3].

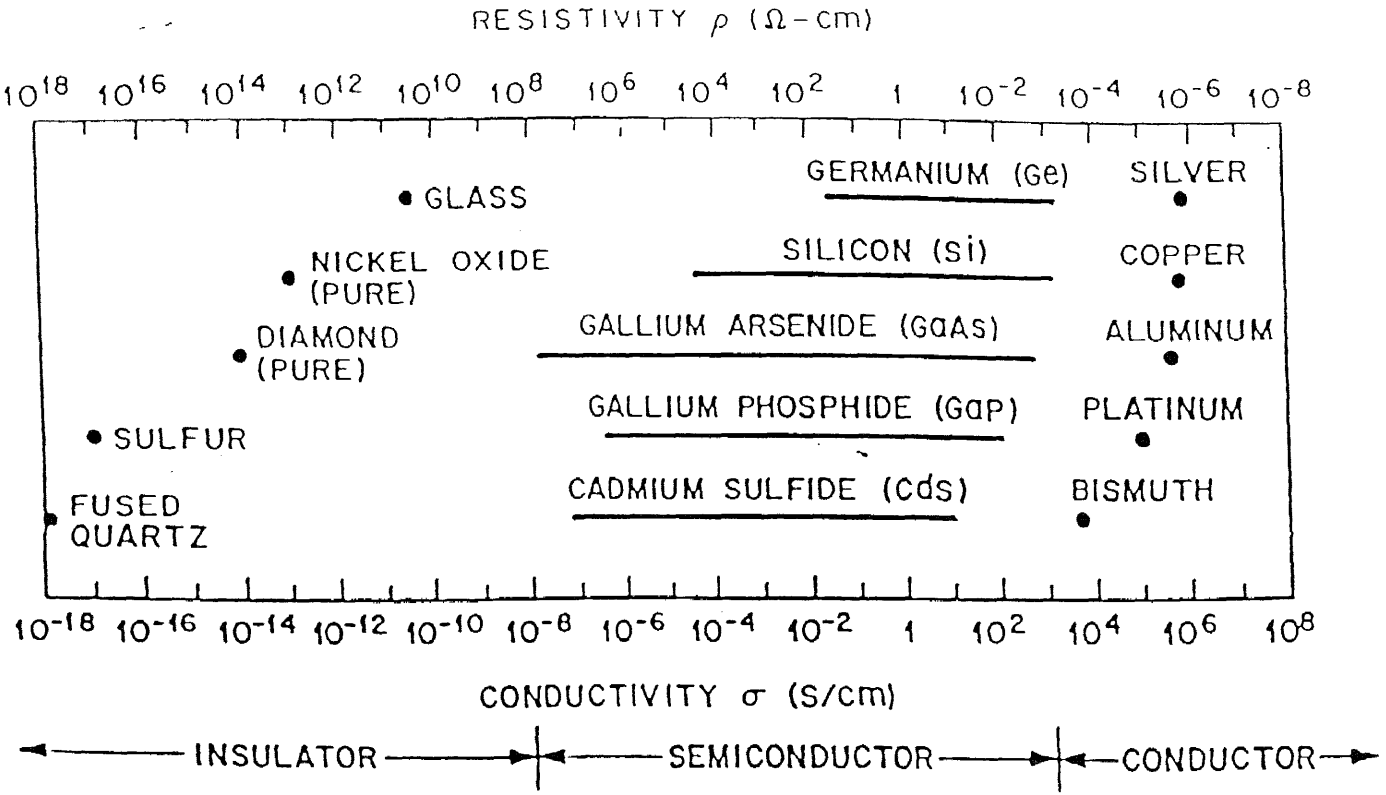

Fig 2.2 Typical range of conductivities for insulators, semiconductors and conductors [3].

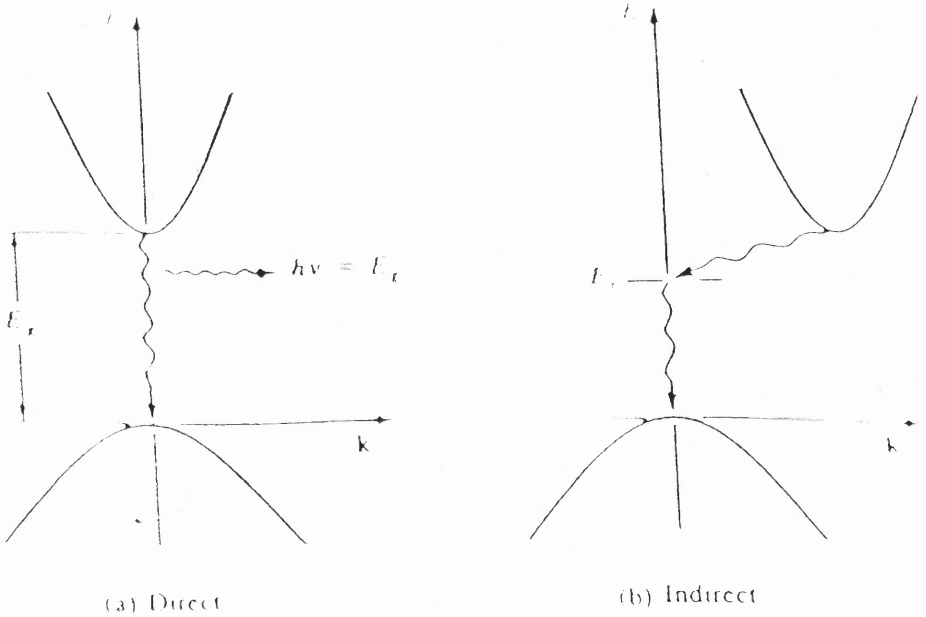

(b)

Fig. 2.4 Direct and Indirect electron transitions in semiconductors [3]

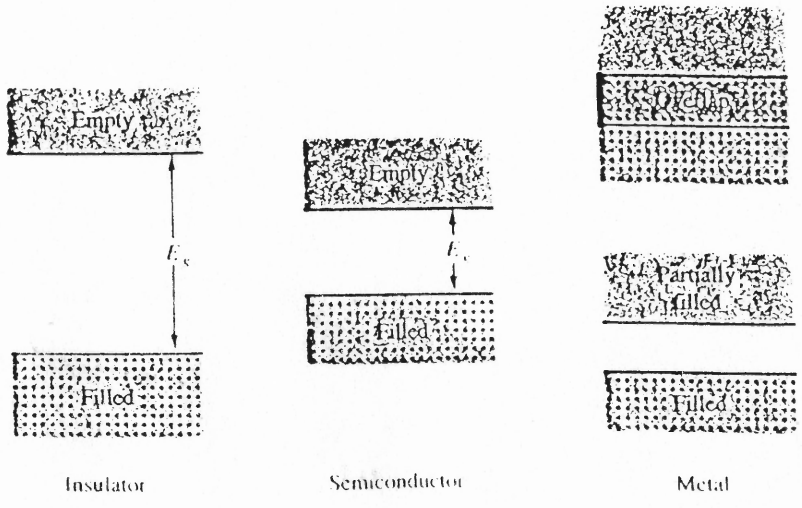

Fig. 2.3 Band structure of metal, semiconductor and insulator at 0 K [3]

television screens usually are II-VI compounds such as ZnS. Photo detectors are commonly made with InSb, CdSe, or other compounds such as PbTe and HgCdTe. Silicon and Ge are also widely used as infrared and nuclear radiation detectors. An important microwave device, the Gunn diode, is usually made of GaAs or InP. Semiconductor lasers are made using GaAs, AlGaAs, and other ternary and quadrinary compounds.

2.1.2 Properties of Semiconductors

Semiconductors are a group of materials having electrical conductivity intermediate between metals and insulators. It is significant that the conductivity of these materials can be varied over orders of magnitude by changing the temperature, optical excitation and impurity content. The electronic and optical properties of semiconductor materials are strongly affected by impurities, which may be added in precisely controlled amounts. Such impurities are used to vary the conductivity of semiconductors over a wide range and even to alter the nature of the conduction process. For example, an impurity concentration of one part per million can change a sample of silicon from poor conductor to a good conductor of electric current. This process of controlled addition of impurities is called *doping*.

Another important characteristic of a semiconductor, which distinguishes it from metals and insulators, is its energy gap. Semiconductor materials at 0 K have the same structure as insulator- a filled valence band separated from an empty conduction band. The difference lies in the size of the band gap E_g, which is much smaller in semiconductors than in insulators. The relatively small band gaps of semiconductors

allow for excitation of electrons from the lower (valence) band to the upper (conduction) band by reasonable amounts of thermal or optical energy. For example, at room temperature, a semiconductor with a 1eV band gap will have a significant number of electrons excited thermally across the energy gap into the conduction band, whereas an insulator with 10eV bandgap will have a negligible number of excitations. An important difference between semiconductors and insulators is that the number of electrons available for conduction can be increased greatly in semiconductors by thermal or optical energy.

As the temperature of a semiconductor is raised from 0K, some electrons in the valence band receive enough thermal energy to be excited across the band gap to the conduction band. The result is a material with some electrons in an otherwise empty conduction band and some unoccupied states in an otherwise valence band. For convenience, an empty state in the valence band is referred to as *hole.* If the conduction band electron and the hole are created by excitation of a valence band electron to the conduction band, they are called an electron-hole pair (EHP). There are two classes of semiconductor energy bands: direct and indirect. Here, allowed values of energy can be plotted vs. propagation constant 'k'. An indirect transition involves a change in momentum for electron.

2.2 Summary of Properties of Silicon

2.2.1 Material Properties

Although many elements and intermetallic compounds exhibit semiconducting properties, silicon is used almost exclusively in the fabrication of semiconductor devices and microcircuits.

Of many reasons for this choice, the most important are the following: (a) Silicon is an elemental semiconductor. It can be subjected to a large variety of processing steps without the problem of decomposition that are ever present with compound semiconductors, (b) Consequently it can be fabricated into microcircuits capable of operation at higher temperatures. At the present time, the upper operating temperature for silicon microcircuits is between 125^0 C to 175^0 C, which is entirely acceptable for both commercial and military applications, (c) Silicon lends itself readily to surface passivation treatments. This takes the form of a layer of thermally grown SiO_2 which provides a high degree of protection to the underlying device.

The fabrication of devices such as metal-oxide-semiconductor (MOS) transistors has emphasized that SiO_2 provides the best possible control of surface phenomena. Because of the above, a significant technological base has been established to take advantage of its characteristics.This includes the development of a number of advanced processes for deposition and doping of silicon layers, as well as sophisticated equipment for forming and defining intricate patterns for very large scale integration (VLSI). Although silicon is the workhorse of the semiconductor industry, it is not an optimum choice in every respect. Indirect band-gap does not allow many functions to be performed by silicon. These include transferred electron oscillators, lasers, light-emitting devices

and a variety of highly efficient, lightweight, photovoltaic devices for space as well as terrestrial applications.

2.2.2 Physical Properties

In single-crystal form, silicon adopts the diamond lattice structure, with 5.2 x 10^{22} atoms/cm^3 and each atom covalently bonded to four nearest neighbors. Many of its physical properties result from this strong covalent bonding. In pure form, its lattice constant is 5.43086 Angstroms at 300 K. Thus it is difficult to make silicon semi-insulating(SI).

When thermally oxidized, silicon has a significantly lower density of surface states. The electron mobility of lightly doped silicon is 1350 cm^2/Vs and that of hole mobility is 475 cm^2/Vs at 300 K [4]. Shear stress for silicon is 3.61 x 10^7 dyne cm^{-2} [4]. Due to this property of silicon, it is possible to handle a 300mm wafer. The minimum separation between conduction and valence bands which is the thermal activation energy or the band gap is 1.1eV, but the minimum vertical transition is 2.5eV. As in any semiconductor, the band gap Eg(T) is expected to depend on temperature T, through two effects, lattice dilation and electron-phonon interaction. Direct transitions will thus only be possible with visible photons. Any infrared absorption must arise from indirect transitions.

CHAPTER 3

TEMPERATURE MEASUREMENT TECHNIQUES

In semiconductor processing, it is very important to know the exact temperature of the wafer surface. The non-uniformity of the wafer temperature at various points on the wafer surface forces us to determine the spatial distribution of temperature across the wafer surface. The most widely used measurement techniques to determine temperature in RTP are optical pyrometry and thermocouple embedded wafers.

3.1 Contact Sensors

3.1.1 Thermocouples

Thermocouples are defined as a junction of two dissimilar materials that, upon heating will produce a voltage across the two open leads. This effect is called the thermovoltaic effect. When more than one of the junctions are combined in a single responsive element, it is known as thermopile.

Some of the important features of thermocouples are discussed in this section. Firstly, (a) Thermocouple does not measure the junction temperature, and instead it measures the temperature gradient of the wire. (b) thermocouple does not measure wafer temperature directly. Only a close approximation is the output of the thermocouple, as determined by the thermal resistance between the wafer and the thermocouple. (c) the signal produced by the thermocouple is translated into temperature by a number of methods. The most common conversion is the use of a standard reference table.

3.1.2 Limitations of Thermocouples

In order to measure the temperature of an object, the thermocouple needs to be in physical contact or embedded in the object under investigation. This leads to risk of contamination of the wafer as well as the process chamber. In order to minimize the contamination, real-time measurements must not involve any physical contact with the wafer.

Thermocouples can be used as temperature measurement tools in batch reactor furnaces, where the wafer is in total equilibrium with its sorroundings. By determining the furnace temperature, wafer temperature can be determined. In processes like Rapid thermal processing (RTP), the thermocouple should be embedded inside the wafer in order to determine the wafer temperature since the wafer is not in thermal equilibrium with the furnace temperature. This technique cannot be used in processes such as rapid thermal oxidation (RTO), where a layer of thermal oxide is grown on the surface of the substrate.

Although there are many limitations in using the thermocouples including the associated large time constants, it is unlikely to see the disappearance of thermocouples in the semiconductor industry in the near future.

3.2 Non-Contact Sensors

3.2.1 Pyrometers

Pyrometry is an optical technique that determines the surface temperature of the sample by detecting its radiated flux. Pyrometers consist of responsive elements for IR detection,

software and hardware coupled with them as part of the control system to determine the temperature of the object under investigation.

The responsive element in a pyrometer can be one of the following:

(a) Bolometers: Incident IR photons cause an increase in the bolometer temperature. Since the bolometer resistance versus temperature curve has a non-zero slope, a change in temperature leads to change in the bolometer resistance.

(b) Photoconductive detector: A change in the incident photon flux on the semiconductor surface causes a change in the generated free-carriers, thus, causing a change in the electrical conductivity.

(c) Photoelectromagnetic detector: IR photons absorbed by the detector generate free-carriers which diffuse in the bulk and are separated by a magnetic field. The charge separation causes an electrical signal that is proportional to the number of photons.

(d) Photovoltaic detector: changes in the number of incident photons cause change in the voltage generated by the junction.

(e) Pyroelectric detector: IR photons change the temperature of the crystalline responsive element. This alters the dipole moment, which produces an external electric field.

The change in the number of incident photons, which is a function of the radiating source, causes a change in the electrical signal. Upon monitoring the electrical signal that results in voltage or conductivity change in a coupled electronic circuit and analyzing the resulting I-V curves from the pyrometer, the IR intensity is determined. Thus, for an ultra-clean environment and a tight control over contamination in processes like RTP, pyrometers will be the better choice for temperature measurements and control.

3.2.2 Limitations of Pyrometers

Pyrometers are limited by their operating wavelengths, which can limit sensivity to samples depending on the radiation at that particular wavelength as a function of temperature. Pyrometers are also limited by their spatial resolution, which is a direct function of the exitence detector solid angle.

In RTP, the pyrometers are situated at the lower (or upper) level of the chamber and sometimes at the back of a shield located below the wafer to eliminate stray lamp radiation as in the AG Associated design. In order to determine the accurate temperature of the wafer according to the requirements of the industry, i.e ± 3 degrees, emissivity is the term that will stand out as the most important factor that has to be determined precisely [5,6].

CHAPTER 4

EMISSIVITY AND RADIATIVE PROPERTIES

4.1 Blackbody Radiation

A blackbody is a perfect absorber of electromagnetic energy. The spectrum of radiation emitted from a blackbody is described by the Planck radiation function. Actually, it is the mathematical function for the spectral radiance of blackbodies, and is given by:

$$W_{bb}(\lambda, T) = c1/\lambda^5 \left(\exp\left(c2 / (\lambda T) - 1 \right) \right) \qquad (4.1)$$

where 'W_{bb} (λ, T)' is known as the spectral radial exitence, and describes the power per unit area and wavelength radiated into the forward hemisphere from a blackbody at the absolute temperature T in K , at the wavelenghth 'λ' in μm.

The total energy emitted by a blackbody at any temperature can be found by summing up the energy emitted at each wavelength. The result is that the total energy radiated by a blackbody is proportional to its absolute temperature to the fourth power. This is called the Stefan-Bolzmann radiation law.

$$W_{tot.bb} = \sigma T^4 \qquad (4.2)$$

where Wtot.bb is the power radiated per unit area, 'σ' = 5.67×10^{-8} $Wm^{-2} K^{-4}$ is the Stefan-Bolzmann constant and T is in K.

4.2 Link between Thermal and Radiative Properties

4.2.1 Optical Properties

The optical response of a material can be described using various interrelated properties.The response of a solid to electromagnetic radiation is generally regarded as a

consequence of its microscopic elements with the electric field and hence it can be summarized by defining the dielectric constant ε_r (v), which is a function of the frequency of the wave.

$$\varepsilon_r (v) = \varepsilon_1 (v) + j\, \varepsilon_2 (v) \qquad (4.3)$$

The dielectric constant is not usually measured directly, and a number of other properties are used to describe the optical response of a material. The complex refractive index, n_c, is defined by the relation,

$$n_c = (\varepsilon_r)^{1/2} \qquad (4.4)$$

The complex refractive index can be written as

$$n_c = n + jk \qquad (4.6)$$

where 'n' and 'k' are refractive index & extinction coefficient respectively. The relationships between the dielectric function and "n' and "k" are summarized by the equations,

$$\varepsilon_1 = n^2 - k^2 \qquad (4.7)$$

$$\varepsilon_2 = 2nk \qquad (4.8)$$

The absorption coefficient 'α' is defined as

$$'\alpha' = 4\pi k / \lambda$$

where 'λ' is the wavelength . 'α' is usually expressed in cm^{-1}

4.3 Emissivity

Emissivity is defined as the ratio of the radiation emitted by a wafer with temperature T, at a given wavelength 'λ', angle of incidence 'θ' and the plane of polarization 'φ', to that emitted from a blackbody under the same conditions. It is a function of the azimuthal

angle if the surface does not have azimuthal symmetry. Since this definition is for narrow spectral intervals, it refers to spectral emissivity.

In order to make comparison of emission from materials at various temperatures, we need to remove the temperature effect. This is done mathematically by dividing the radiance spectrum of selective emitters by that of a blackbody (perfect emitter) at the same temperature. This result is called an emissivity spectrum. Emisssivity is a property, which must be known for accurate temperature determination of an object by measurement of its electromagnetic radiation with a radiation thermometer. For RTP, there are three reasons to know wafer emissivity:

1) Pyrometry
2) Thermal modeling
3) For wafer design and construction to test the robustness of an RTP chamber or process.

For normal incidence, the emissivity $\varepsilon(\lambda)$ of a plane parallel specimen is given by :

$$\varepsilon(\lambda) = [1-R(\lambda)]\,[\,1- T(\lambda)]\,/\,[\,1 - R(\lambda)T(\lambda)] \qquad (4.3.1)$$

where 'λ' is the wavelength, $R(\lambda)$ is the true reflectivity and $T(\lambda)$ is the true transmissivity.

$R(\lambda)$ and $T(\lambda)$ are related to the fundamental optical parameters – $n(\lambda)$, the refractive index and $k(\lambda)$, the extinction coefficient by the following relations :

$$R(\lambda) = [\{n(\lambda)- 1\}^2 + k(\lambda)^2]\,/\,[\{n(\lambda)+1\}^2 + k(\lambda)^2] \qquad (4.3.2)$$

$$T(\lambda) = \exp[\,-\alpha(\lambda)t / \lambda\,] = \exp[\,-4\pi\, k(\lambda)t/\lambda\,] \qquad (4.3.3)$$

where 'α' is the absorption coefficient and 't' is the thickness of the material. When the radiant heat transfer is in an equilibrium state, the emissivity of perfectly opaque bodies

is given by Kirchoff's law as 1 - R(λ) for an opaque body, since T(λ) = 0. Therefore we have

$$\varepsilon(\lambda) = [1-R(\lambda)] \qquad (4.3.4)$$

The experimentally measured values of transmittance and reflectance include effects such as light trapping and multiple internal reflections depending on the angle of incidence, surface roughness, presence of grains, grin boundaries, interface roughness etc. These apparent T (λ)* and apparent reflectance R(λ)* are related to real or true transmittance T(λ) and true reflectance R(λ), respectively by the following equation:

$$T(\lambda)^* = T(\lambda) \{ (1- R(\lambda))^2 / (1- R(\lambda))^2 T(\lambda)^2) \} \qquad (4.3.5)$$

$$R(\lambda)^* = R(\lambda) \{ 1 + [T(\lambda)^2 (1- R(\lambda))^2] / [1 + [T(\lambda)^2 (1- R(\lambda))^2] \} \qquad (4.3.6)$$

Equations (4.3.5) and (4.3.6) are the result of considering multiple internal reflections. With the choice of appropriate models, n (λ) and k (λ) of the multilayers can also be resolved from experimentally measured spectral properties. Emissivity models can convey to a process engineer, the nature of the films and film thickness, required to achieve the desired emissivity.

CHAPTER 5

EXPERIMENTAL APPROACH

5.1 Spectral Emissometer

The schematic of the spectral emissometer utilized in this investigation is presented in the Fig. 5.1. The spectral emissometer has been used to measure the optical properties of some silicon related materials. The detailed description, along with its operation, is presented in Appendix I.

This instrument is used to measure the radiative properties of a sample over a wide spectral range, in the near to mid-infrared, from 12,500 cm^{-1} to 500 cm^{-1} (0.8 to 20μm). It consists of a hemi-ellipsoidal mirror providing two foci, one for the exciting source in the form of a diffuse radiating near blackbody source and the other for the sample under investigation. A microprocessor controlled motorized chopper facilitates in simultaneous measurement of sample spectral properties such as reflectance, transmittance and emissivity.

The Fourier transform infrared (FTIR) data collection system consisting of Ge (0.8-1.6μm) and HgCdTe (1.6-20μm) detector, is synchronized with the two sets of the chopper allowing for the distinction of the sample radiation from reflected/transmitted radiation. A carefully adjusted set of five mirrors provide the optical path for the measurement of the optical properties. The source of heating of the samples is provided by an oxy-acetylene/propane torch. A high resolution Bomem FTIR detector, interfaced with a Pentium proccesor, permits the data acquisition of the measured optical properties.

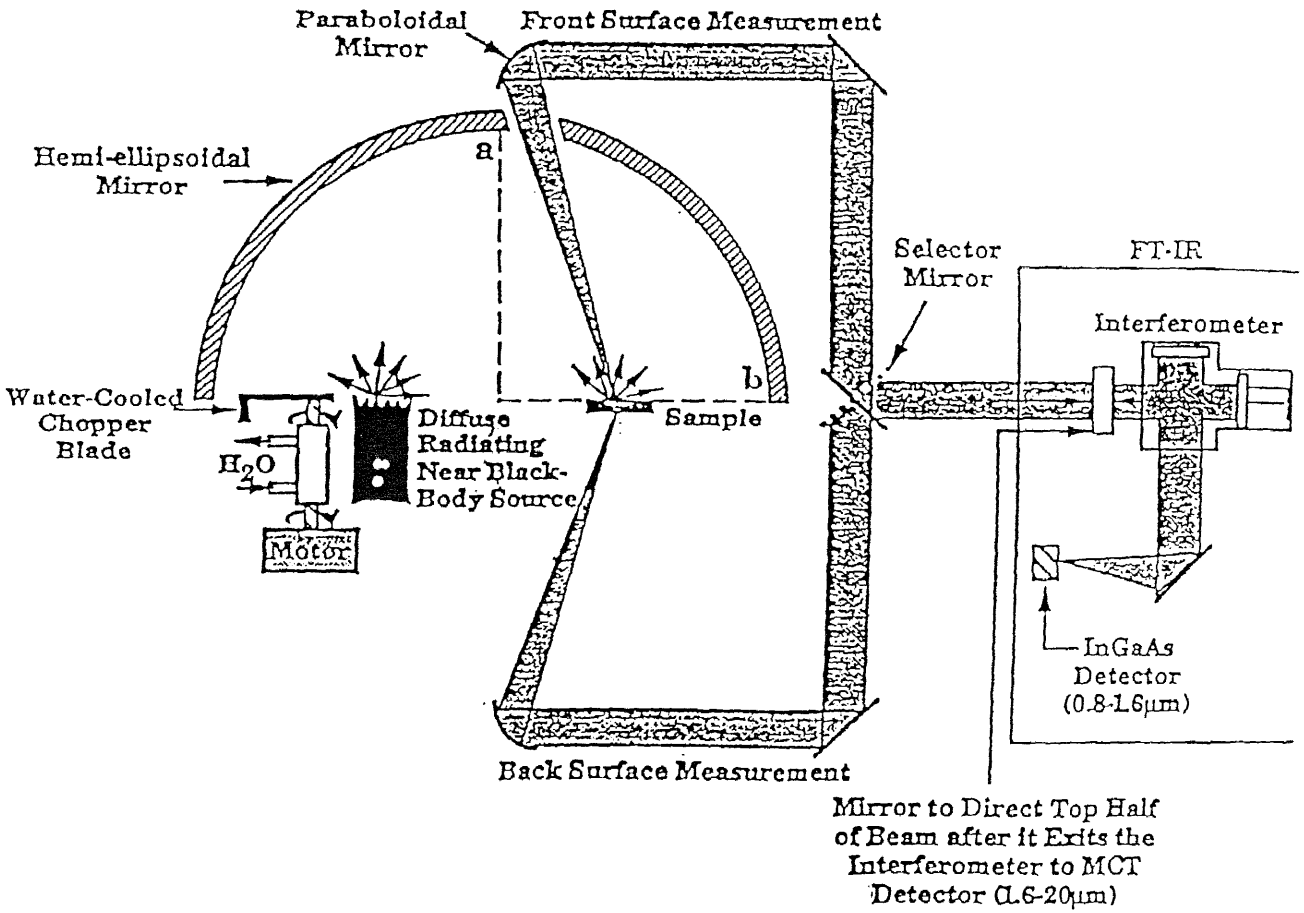

Fig. 5.1 Schematic of Benchtop Emmisometer [7]

This on-line computer enables the user to flip the mirror to acquire transmission/reflection via a software Spectra Calc. This instrument has applications for : (1) industrial quality control of radiative properties of processed materials, (2) research and development of new materials and temperature measurements by optical techniques in the near and mid IR.

5.2 Theory

The spectral emissometer allows for simultaneous measurements of radiance, reflectance, transmittance and the temperature of the sample at the measured point.The theoretical backround and the methodology are as follows :

The sample is placed at one of the foci of the hemispherical ellipsoidal mirror while the source, a blackbody at 900 ^{0}C, is at the other foci. The chopper permits the simultaneous acquisition of the radiative properties of interest including the sample temperature. A front-surface sample measurement, with the chopper closed, yields the sample's directional spectral radiance :

$$Mo\ (closed) = BR_v(T) = B\varepsilon_v(T)\ R_v^b(T) \qquad (5.1)$$

where in $B = A\ dv\ d\Omega\ \cos\theta$, we lump together various factors fixed by the experimental situation; dv is the frequency interval, $d\Omega$ is the solid angle, and A is the sample area at

angle θ with respect to the given direction. $\varepsilon_v(T)$ is the emissivity of the sample at temperature T, and R_v^b is the blackbody radiance.

Radiance $R_v^b(T)$ is defined as the rate that energy is radiated at frequency 'v' from a blackbody at temperature 'T' per unit frequency per unit solid angle per unit normal area.

When the chopper is open, the measured radiation is given by,

$$Mo\ (open) = R_v(T) + \rho_v(T)\, R^b_v(T_{bb}) \qquad (5.2)$$

Where , T_{bb} is the constant blackbody source temperature which is maintained at 900 ^{0}C and ρ_v is the spectral directional-hemispherical reflectivity. The difference in the two measurements yields $\rho_v(T)\, R^b_v(T_{bb})$.

$$Mo\ (open) - R_v(T) = \rho_v(T)\, R^b_v(T_{bb}). \qquad (5.3)$$

The constant source radiation is quantified by replacing the sample with the perfect reflector (a gold mirror, $\rho_v^{\ gold}(T) = 1.0$) and measuring the spectrum in the chopper open condition.

$$M_v^{ref} = \rho_v^{\ gold}(T)\ R^b_v(T_{bb}) = R^b_v(T_{bb}) \qquad (5.4)$$

The ratio of equations (5.3) to (5.4) results in the measurement of the directional hemispherical reflectance of the sample ρ_v , at the unknown temperature T.

$$Mo\ (open) - R_v(T) / M_v^{ref} = \rho_v(T)\, R^b_v(T_{bb}) / R^b_v(T_{bb}) \qquad (5.5)$$

For an opaque sample, the spectral emittance ε_v, can be determined from $\varepsilon_v = 1 - \rho_v$

Once the spectral emissivity is known, the precise sample temperature can be determined by rearranging equation (5.1)

$$R^{b}_{\nu}(T) = R_{\nu}(T) / \varepsilon_{\nu}(T) \qquad (5.6)$$

Comparing (5.6) with Planck function leads to temperature evaluation :

$$R^{b}_{\lambda} = c_1 \lambda^{-5} / \exp \{ (c2 / \lambda T) - 1 \} \qquad (5.7)$$

where c_1 and c_2 are constants.

An on – line computer does all the mathematical operations on the raw data using Spectra calc. It transforms the interferograms into spectra, calculates spectral emittance from reflectance and transmittance data and automatically determines the temperature from the radiance data.

CHAPTER 6

RESULTS AND DISCUSSION

6.1 Silicon

The application of spectral emissometry to measure emissivity as a function of wavelength and temperature for some silicon related materials are illustrated in the first part of this chapter.

While the measurements are performed on a variety of samples, the results of measurements on p-type silicon, with front side polished, as a function of wavenumber for temperatures in the range 35°C to 911°C, are presented in Fig.6.1, 6.2 and 6.3 respectively. These wafers have resistivities in the range of 1-2 x 10^{-2} Ω-cm. The observed sharp features in the infra - red spectra in the wavelength range of 1 μm (10000 cm^{-1}) to 20 μm (500 cm^{-1}) are due to the presence of the following infra-red sensitive molecules : (a) C in Si (b) SiO_2 (c) interstitial oxygen in Si (d) water (e) CO_2 . The narrow - band features below 1000 cm^{-1} (10μm) are due to lattice vibrations in silicon. The spectrum in Fig. 6.3, at 213 °C was measured after heating the wafer to the maximum temperature of 911°C. Comparison of the emittance spectrum in these figures indicates reversibility in emittance changes.

A similar measurement on a double side polished n-type wafer exhibits different radiative properties. The emissivity of this wafer is negligible at room temperatures while at high temperatures, it approaches that of single side polished silicon. The most change in this measurement is the loss of transmissivity at elevated temperatures, due to increase in free carrier density, with increase in temperature [8].

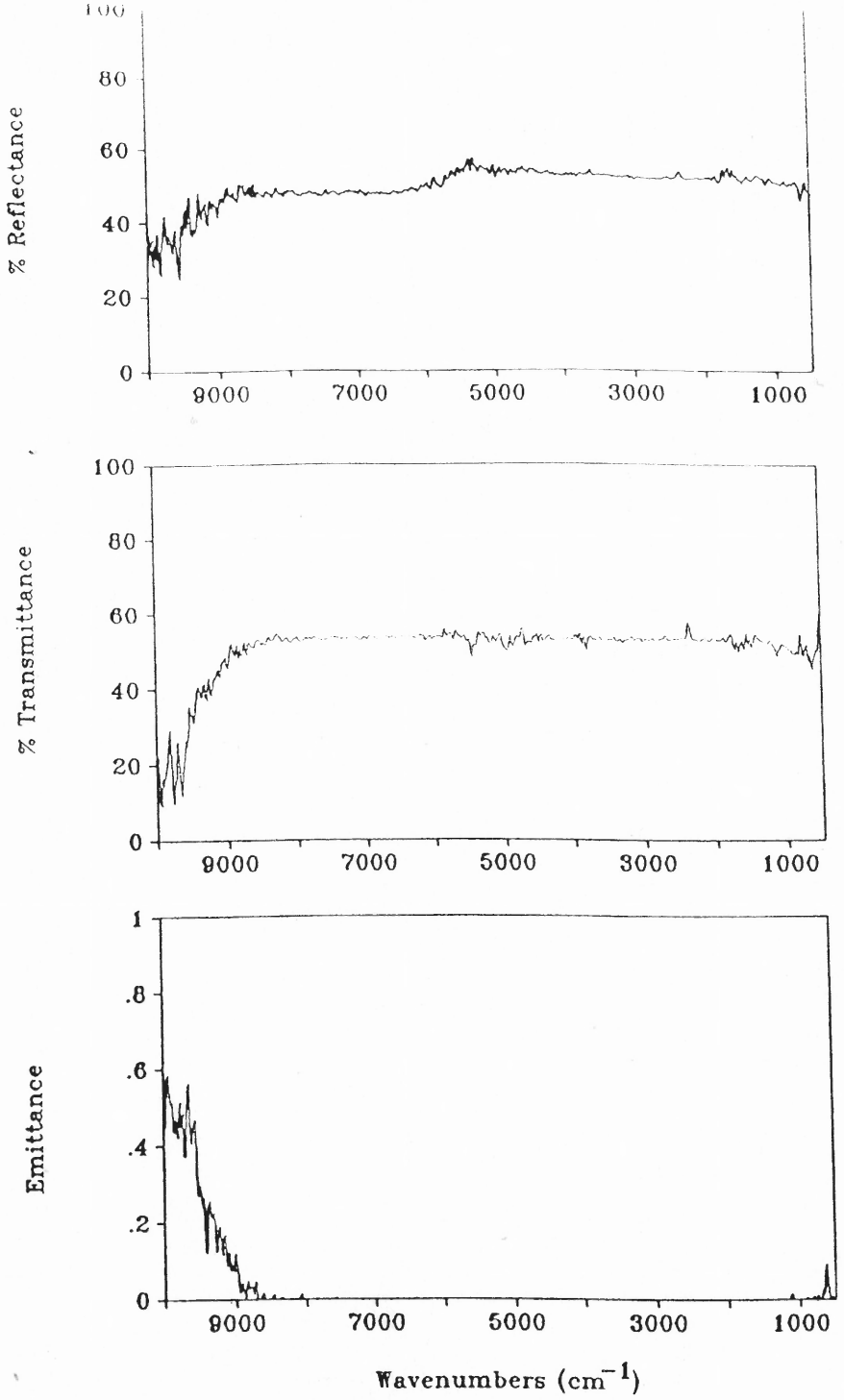

Fig 6 1 Reflectance, Transmittance, and Emittance of p-type silicon wafer at room temperature

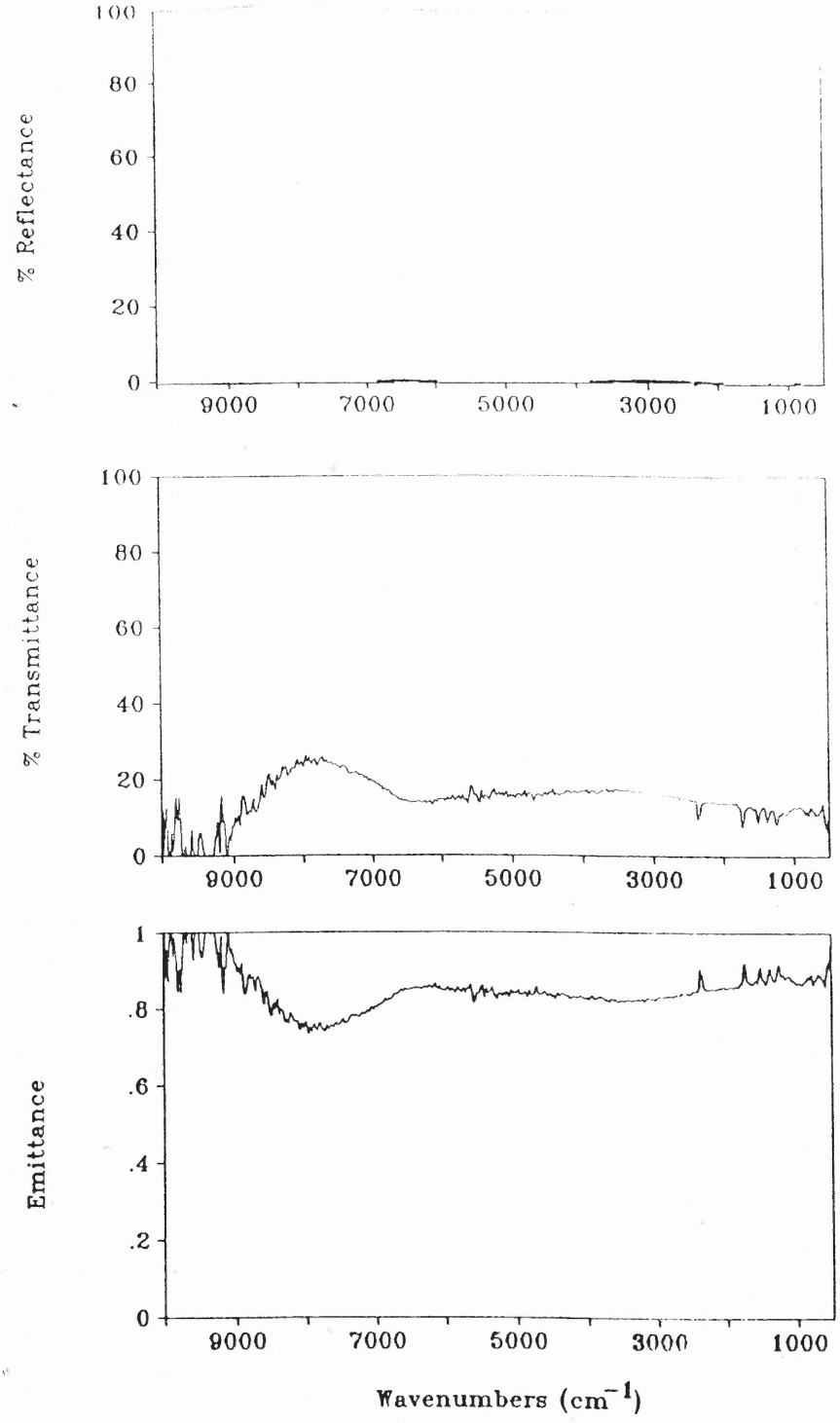

Fig. 6.2 Reflectance, Transmittance, and Emittance of p-type silicon wafer at 911 °C

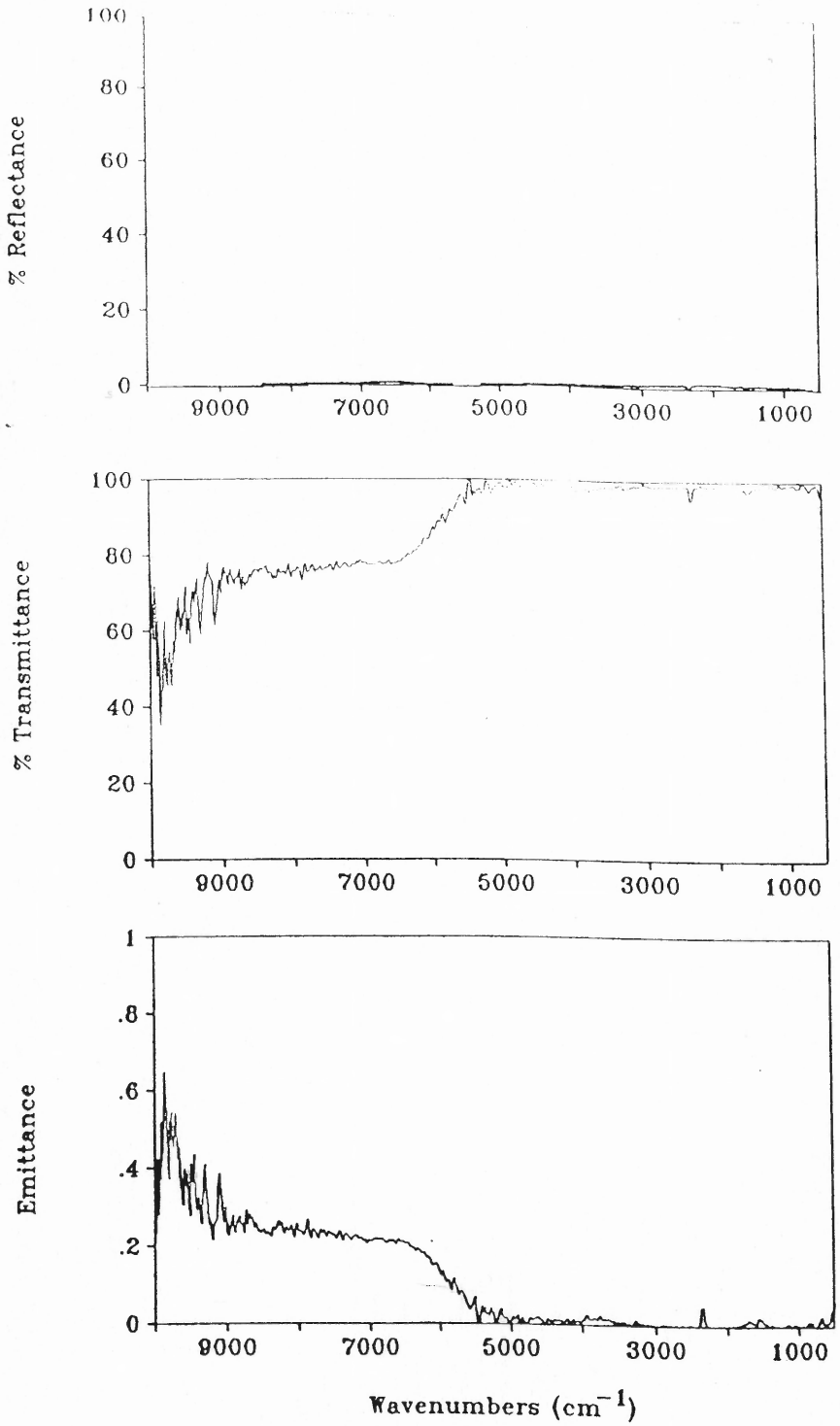

Fig. 6.3 Reflectance, Transmittance, and Emittance of p-type silicon wafer at 213 °C

The total contribution to emissivity, $\varepsilon(\lambda,T)$ is given by,

$$\varepsilon(\lambda,T)_{total} = \varepsilon(\lambda,T)_{free\ carrier} + \varepsilon(\lambda,T)_{as.\ edge} + \varepsilon(\lambda,T)_{phonon} \qquad (6.1)$$

for photon energy, E_{photon} greater or equal to E_g, where E_g is the bandgap, i.e., λ_{photon} lesser or equal to λ_E , the wavelength corresponding to absorption edge ; emissivity contributions are due to bandgap and above bandgap absorption. For $E_{photon} < E_g$, the emissivity contributions are due to below bandgap absorption. The free carrier absorption mechanism plays the dominant role in doped semiconductors in the short – wavelength range. In the long – wavelength range (> 10μm), the phonons contribute to emissivity changes. These properties are function of temperature.

In general, results of the temperature and wavelength dependent emissivity of silicon led to the following observations : (a) The effect of doping, in general, is to reduce the transmittance. Thus intrinsic silicon exhibits high transmittance. (b) As temperature increases, silicon becomes opaque. This facilitates in designing heating sources (contact or noncontact) to measure high temperature optical properties of silicon. Unlike pure silicon, the effect of free carriers/doping is to reduce the emissivity of silicon with increasing temperature. (c) Double side polished wafers seem to show unusually low emissivities at low temperatures.

In the silicon industry, manufacturers of commercial RTP systems have chosen pyrometers to operate at five specific wavelengths – 0.95, 2.5, 2.7, 3.3 and 4.5μm. It is interesting to note that at temperatures above 600 °C, the emissivity is independent of temperature and wavelength.

Table of simulated values of emissivity of Silicon

(t = 700 microns, N = 1.33 X 10 e +14, boron doped)

W/length (μm)	0.8	2.2	2.7	3.4	4.5
Temp(K)					
300	0.663	0.006	0.009	0.009	0.023
400	0.66	0.065	0.076	0.107	0.182
500	0.657	0.238	0.386	0.49	0.536
600	0.654	0.566	0.608	0.673	0.684
700	0.651	0.676	0.682	0.684	0.685
800	0.648	0.678	0.68	0.682	0.684
900	0.645	0.676	0.679	0.682	0.685

6.1.1 Modeling

In order to interpret the above experimental results, a detailed application of the matrix theory, developed by Abeles [11] has been utilized. In this method, the layers are not separable from each other and the full stack comprising of the wafer is treated as a single medium with a certain characteristic matrix. A software package, Multi-Rad, based on the Abeles matrix theory and developed by MIT/SEMATECH [12] has been deployed extensively to compare the theoretical results with the experimental data. The detailed description of this software package is given in Appendix II. This model requires pre-knowledge of the individual layer thickness and the optical constants, such as resitivity, doping type, wavelength and temperature-dependent refractive index and extinction coefficient.

The Multi-Rad model adds the phonon absorption component to the Abeles matrix theory. In addition, this model includes the database of the temperature, wavelength and dopant concentration dependent optical constants that are available in the literature. The observed differences between the measured aand the simulated spectra could be attributed to slight differences in the extinction coefficient and its temperature dependence.

The temperature and wavelength dependence of the front-side emittance of SIMOX, at selected wavelengths, is presented in Table 6.2. The experimental values of emittance are tabulated for specific wavelengths (λ = 0.95, 1.1, 2.2, 2.7, 3.3, 4.5 μm) as a function of temperature. The simulated values are presented in Table 6.2. These are

the standard operating wavelengths for pyrometers that are used for process applications, such as rapid thermal processing (RTP).

6.1.2 Noncontact Methods of Heating

Since silicon is transparent below 600 °C, several approaches are being investigated to establish noncontact and noninterfering methods of heating silicon so that a reliable temperature-dependent study of the optical properties may be performed. These methods include the use of lamps, lasers, e-beams, and flames. The anticipation is that the heat source signal can be completely eliminated in the measurement process. The present approach of using flames is appropriate for the measurement technique since the infrared spectra of the flames are very well known. On the other hand, flames will invariably modify the surface conditions of the samples under study. Ideally, the method of choice would be the one that does not modify the surface and bulk composition of the material at the same time permitting the required optics to measure the radiance from all possible angles [9].

6.2 SIMOX

In Fig. 6.4, the measured front side reflectance, transmittance and emittance of the SIMOX sample has been presented for room temperature.

The SIMOX samples exhibit high reflectance compared to that of bare silicon. Even though silicon comprises more than 99 % of this sample, the results turn out to be totally different from that of bare silicon. In the SIMOX case and particularly at room temperature, i.e., Fig. 6.4, the emittance and transmittance of the sample depend strongly

on the reflectance which depends critically on the thickness of the top two thin film layers - silicon and silicon oxide respectively. The average reflectance for SIMOX is higher than that of bare silicon. However for the back side, we see a decrease in the intensity maxima of the reflectance spectra. This can be attributed to attenuation of the infra-red photons due to the presence of the thick 700μm silicon substrate.

The emittance of SIMOX at room temperature is typical of silicon. At higher temperatures, its emittance increases and is determined by the trend in the reflectance spectra. At these temperatures, where free absorption is the dominant mechanism in silicon, SIMOX differs from silicon. The buried oxide reflects the infra-red photons in this wavelength range preventing increased absorption and hence the decrease in its emittance [10].

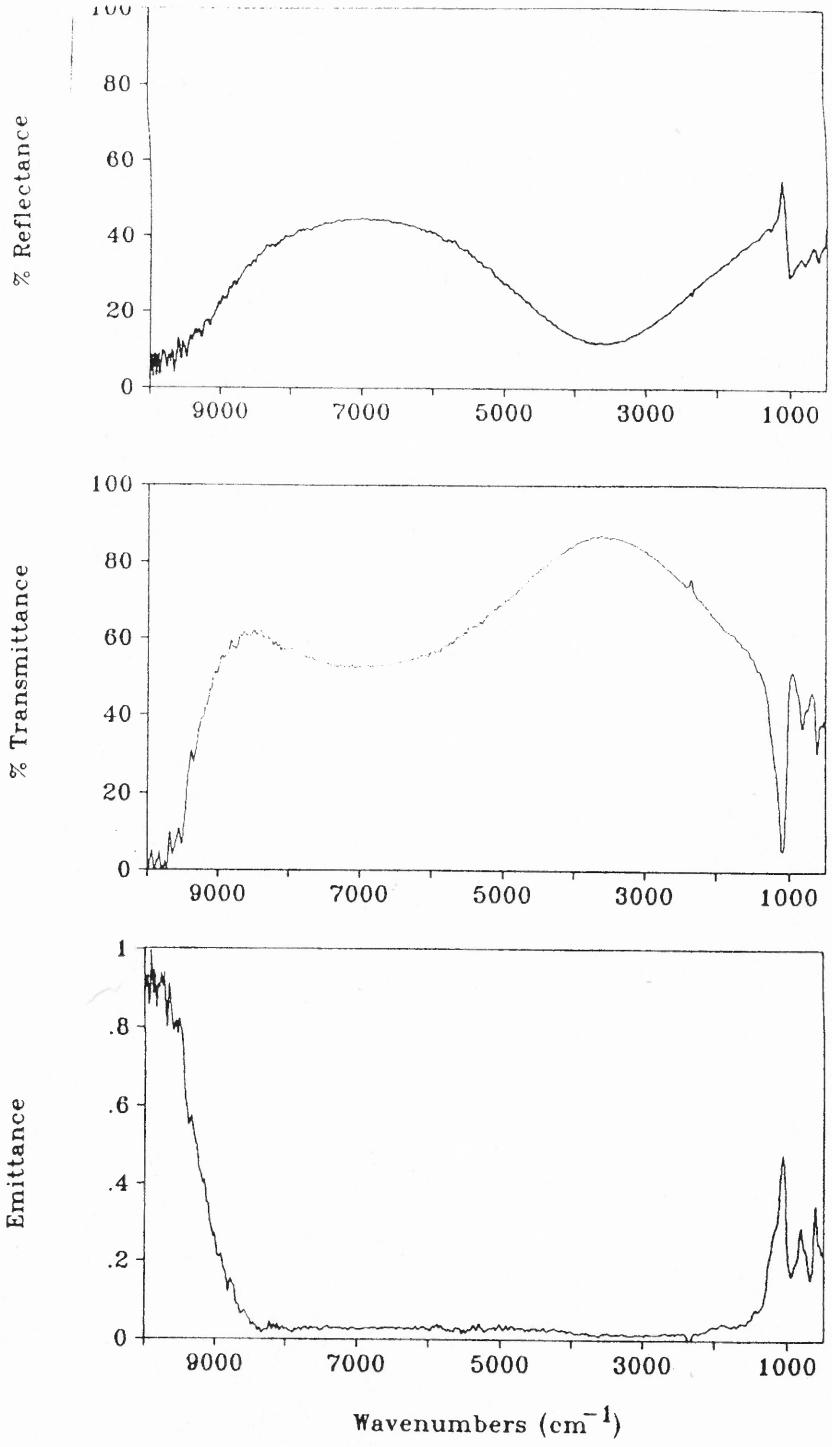

Fig. 6.4 Reflectance, Transmittance, and Emittance of SIMOX wafer at room temperature

Table of Experimental Values of Emissivity for SIMOX

wavelength	micro-m	0.8	0.95	1.1	2.2	2.7	3.4	4.5
Temp.(K)					EMISSIVITY			
303		0	0.32	0.721	0.002	0.002	0.005	0.014
435		1.218	0.3	0	0.014	0	0.0141	0
714		0.42	0	0.709	0	0.088	0	0.332
820		1.386	0.338	0.678	0.201	0.169	0.228	0.372
1084		2.356	0.35	0	0	0	0.235	0
1227		1.431	0.0107	0.224	0.264	0.267	0	0.274
1111		0.754	0	0.251	0.262	0.268	0.2821	0
535		0	0	0.07	0.198	0.1844	0	0.207

Simulated values of SIMOX (Si / Si02 / Si)

W/length	**0.8**	**1.1**	**2.2**	**2.7**	**3.4**	**4.5**
Temp.(K)						
300	0.557	0.721	0.002	0.002	0.005	0.014
400	0.594	0.713	0.014	0.017	0.0141	0.102
500	0.646	0.709	0.072	0.088	0.145	0.332
700	0.709	0.678	0.201	0.169	0.228	0.372
900	0.767	0.644	0.205	0.171	0.235	0.463

6.3 Tantalum

Tantalum is one of the most versatile corrosion resistant metals. The tantalum metal has oxidation characteristics very similar to those of molybdenum in that an adherent oxide of a protective nature cannot be produced at high temperatures [13].

The curves of the Fig.6.5 show the results obtained when polished specimens of tantalum were measured at room temperature. The temperature dependent emissivity of tantalum has been reported in the literature [13]. At higher temperatures, the emissivity increased rapidly until a maximum point was reached, after which an equally rapid decrease occurred. This decrease was caused by an increasing thickness of a white crystalline oxide which was very porous and very nonadherent. Although the emissivity appears to be approaching a stable value, the looseness of the oxide formed precludes any practical uses for this oxide-coated material [13].

Measurements of total hemispherical emissivity of several stable oxidized materials indicate the difficulty in making general conclusions for groups of materials. The manner in which oxidation affects the emissivity may also vary greatly for different metals. The emissivity of most metals increases with an increase in temperature. Finally, the increase in emissivity of an oxidized metal depends largely on the thickness of the coating necessary for stable emissivity. A comparison with the emissivity plots from the literature are presented in the Fig. 6.6.

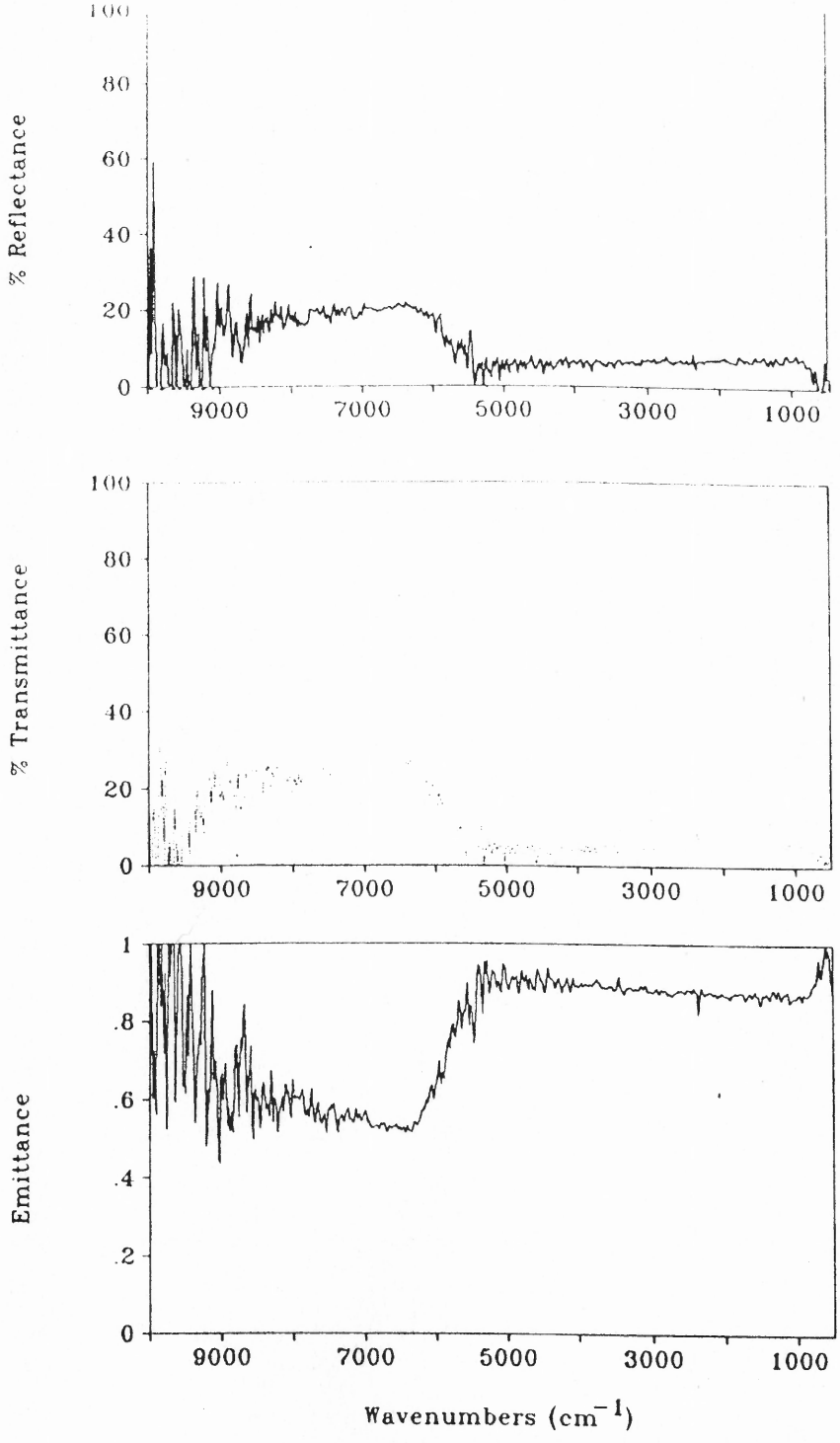

Fig. 6.5 Reflectance, Transmittance, and Emittance of Tantalum wafer at room temperature

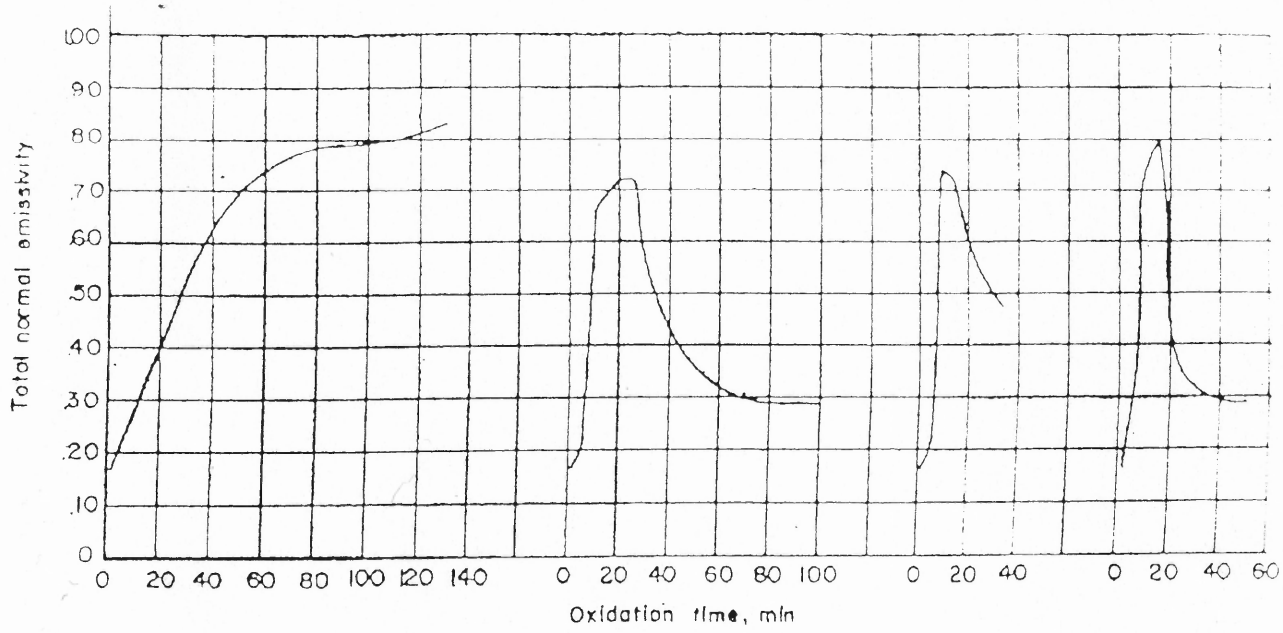

Fig.6.6 Plot of the total normal emissivity of initially polished tantalum wafer from literature [15]

Table of Experimental Values of Emissivity for Tantalum

wavelength (μm)	1.1	2.2	2.7	3.4	4.5
Temp.(K)	EMISSIVITY				
303	0.18	0.0097	0.001	0.001	0.07
435	0	0.014	0	0.0141	0.09
714	0.69	0	0.3	0	0
820	0.56	0.19	0	0	0.1
1084	0	0.26	0.35	0.235	0
1227	0.224	0	0.274	0	0.2
1111	0	0	0	0.2	0
535	0.04	0.198	0.207	0	0.18

CHAPTER 7

CONCLUSIONS

The experimental results show that the measurement of high temperature radiative properties over the wavelength range of 1 to 20 microns and temperature range of 300K to 2000K can be performed using a novel approach based on the use of a spectral emissometer. Methodology of obtaining temperature from simultaneous measurement of reflectance, transmittance and radiance has been shown with applications to silicon, SIMOX and Tantalum.

Results of the temperature and wavelength dependent emissivity of silicon related materials from the spectral emissometer were compared with the simulation software, Multi-Rad (developed by MIT/SEMATECH). The temperature measurement accuracy, with the emissometer, was found to be within $\pm 10\ ^{\circ}$ C of the thermocouple temperature in the temperature range of 30 $^{\circ}$ C to 300 $^{\circ}$ C. The results lead to the following observations:

- The effect of doping in general is to reduce the transmittance. Thus, intrinsic Si exhibits high transmittance.
- The silicon sample becomes opaque as temperature increases. This characteristic is critical in designing heating sources (contact or non-contact) to measure high temperature optical properties of silicon.

Simulation results show the variation in emissivity with respect to the buried oxide in SIMOX.

Recommendations :

Spectral emissometer has thus been established as a reliable technique for simulataneous measurement of temperature and optical properties of semiconductors. In order to make the technique user friendly, following suggestions could be incorporated :

Silicon is transparent below 600° C, several approaches are being investigated to establish noncontact and noninterfering methods of heating silicon so that reliable temperature dependent study of the optical properties may be performed. These methods include the use of lamps, lasers, e-beams and flames.The heat source signal can be completely eliminated in the measurement process. The present approach of using flames is appropriate for the measurement technique since the infrared spectra of the flames are very well known. The flames will invariably modify the surface conditions o the samples under study. The method of choice would be the one that does not modify the surface and bulk composition of the material at the same time permitting the required optics to measure the radiance from all possible angles. A sample chamber with a controlled environment would be very useful in keeping the measurement process and surface conditions of the samples free of contaminants.

APPENDIX I

SPECTRAL EMISSOMETER

- **Instrument Function**

The AFR Emissometer measures radiance, directional-hemispherical reflectance, and directional-hemispherical transmittance from materials at elevated temperatures from 100 degrees to 2000 degrees. The instrument measures these radiative properties over a wide spectral range, in the near and mid-IR, from 11,100 cm^{-1} to 500 cm^{-1} (0.9 to 20 μm). These measurements are then processed to determine the spectral emittance of the material and the temperature at the point of measurement. The instrument has applications for : (1) industrial quality control of radiative properties of processed materials ; (2) research and development of new materials; (3) temperature measurement by optical techniques in the near and mid-IR ; aand (4) determination of heat transfer properties of materials.

- **Bomem / Hartman & Braun Model 155 FT-IR Spectrometer**

The spectrometer used in the system is a Fourier Transform Infrared Spectrometer. This instrument does not measure a spectrum directly, but an interferogram, which has to be Fourier transformed to yield the spectrum. The spectral resolution is variable in the system. The FT-IR spectrometer is utilized in emission mode, and can accept radiation from either side of the sample by positioning the select mirror. The design of Bomem's interferometer allows the incoming beam to be modulated and then split into two beams of identical information. In the emissometer, two separate detectors are utilized to

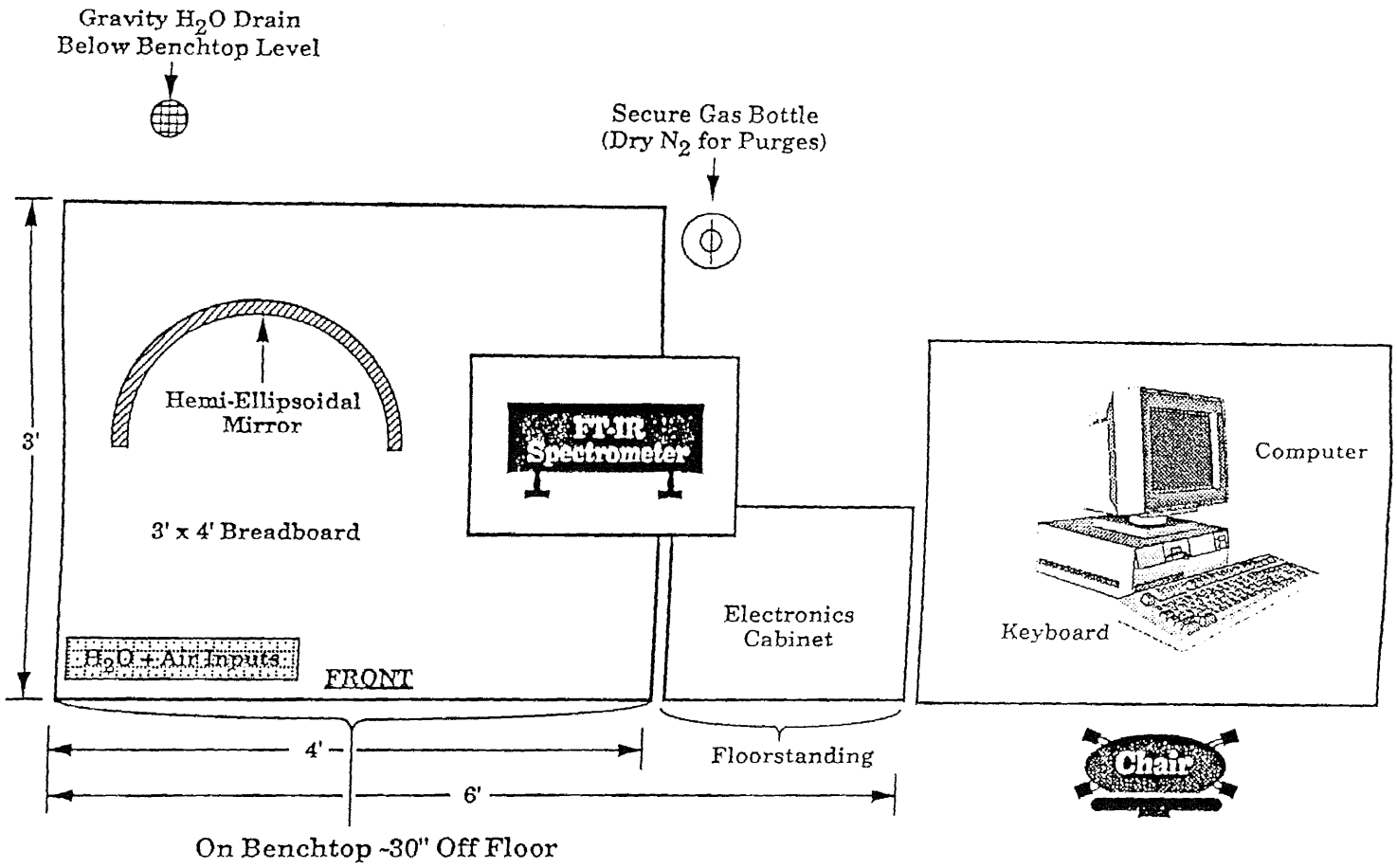

Figure 2.1. Suggested Work Space Configuration for AFR Emissometer

measure near and mid-IR energy. A room temperature germanium (Ge) detector is sensitive to near-IR energy (0.9 –1.6μm) and a liquid nitrogen cooled mercury-cadmium-telluride (MCT) detector is sensitive to longer wavelengths (1.6 to 20 μm). Both the spectral regions are measured simulataneously.

- **Emissometer Optical Bench**

The breadboard optical bench supports : (1) the FT-IR spectrometer elevated on a platform ; (2) the hemi-ellipsoidal mirror in a support housing ; (3) mirrors on supports for the near-IR and mid-IR energy transfer; (4) sample, source, and calibration furnace holders ; (5) the water cooled chopper assembly (6) water and air-flow controllers; and (7) holders for different techniques of sample heating.

- **Electronics Cabinet**

The Electronics rack houses : (1) the circuitry for chopper speed control and synchronistic motion with FT-IR data collection ; (2) electronic temperature controllers for the control of calibration furnace , and source ; (3) thermocouple connections ; (4) variable output transformers for voltage supply to calibration furnace and source ; (5) interface board for computer control of beam path selector mirror.

- **Computer and Data Acquisition**

The computer does all mathematical operations required on the raw data. It transforms the interferograms into spectra, calculates spectral emittance from reflection and

transmission data, and automatically determines temperature from radiance data which is normalized by emittance.

- **Procedure for Data Conversion**

The procedure that is followed for the conversion, from the raw data detected, to the tabulated data is as follows :

a) The particular file used for data acquisition is re-opened in GRAMS software.

b) A plot of the acquired data is made.

c) A single-click on the plot allows the user to paste the data in tabular form in a work-sheet.

d) The data is re-arranged and presented in a tabular form.

APPENDIX II

MULTI-RAD

- **Introduction**

Multi-Rad, developed by MIT/SEMATECH, is a PC based software that calculates the radiative properties of thin-film stacks, with emphasis on semiconductor applications. The model assumes that the layers are optically smooth and parallel, and the materials are optically isotropic (the optical constants are not dependent on crystollographic orientation). Therefore, the theory does not predict any variation of properties in the azimuthal direction. For a given multi-layer stack at a prescribed temperature, the user can calculate the radiative properties as they vary with wavelength and angle of incidence.

- **Spectral Analysis**

The method used to calculate the radiative properties is thin film optics, implemented in the form of matrix method of multilayers. This theory assumes that the interfaces are optically smooth and parallel, and provides the spectral directional radiative properties.

Angle of Incidence

The program assumes that there is no variation in properties over azimuthal angle.

Single : This will do a calculation for a single angle of incidence. Normal incidence is zero degrees, grazing incidence is 90 degrees.

Range : This option allows the user to select a range of agles of incidence, over which the spectral properties will be integrated. For example, choosing 0 to 90 will yield an integration over the whole hemisphere (spectral hemispherical properties). Integration over the whole hemishere will increase the calculation time by approximately a factor of 25, relative to a sigle angle calculation. Calculation time decreases with decreasing size of the range.

- **Spectral Range**

Min / Max : This dictates the spectral range over which you want to calculate properties. This limits must be between 0.4 and 20.0 μm.

Increment : This dictates the increment that the calculation will be done for. The minimum increment is 0.001 μm. The smaller the increment, the more calculated data points, and so the longer the calculation will take.

- **Calculation**

Once the angle of incidence, spectral range and stack are defined, the calcualtion for the required optical properties are done. Once the calculations are done, the results are displayed in the tabular form in the output form in the output box. In most situations, including rapid thermal processing, the spectral absorptance is equal to the spectral emittance.

- **Plotting**

Once the data is calculated, an x-y plot of the properties can be done. A dialogue box allows the user to choose the plotted variable, and the limits for the spectral range and the plotted range. An example of the simulated output of Multi-Rad is shown in Fig. A2.1

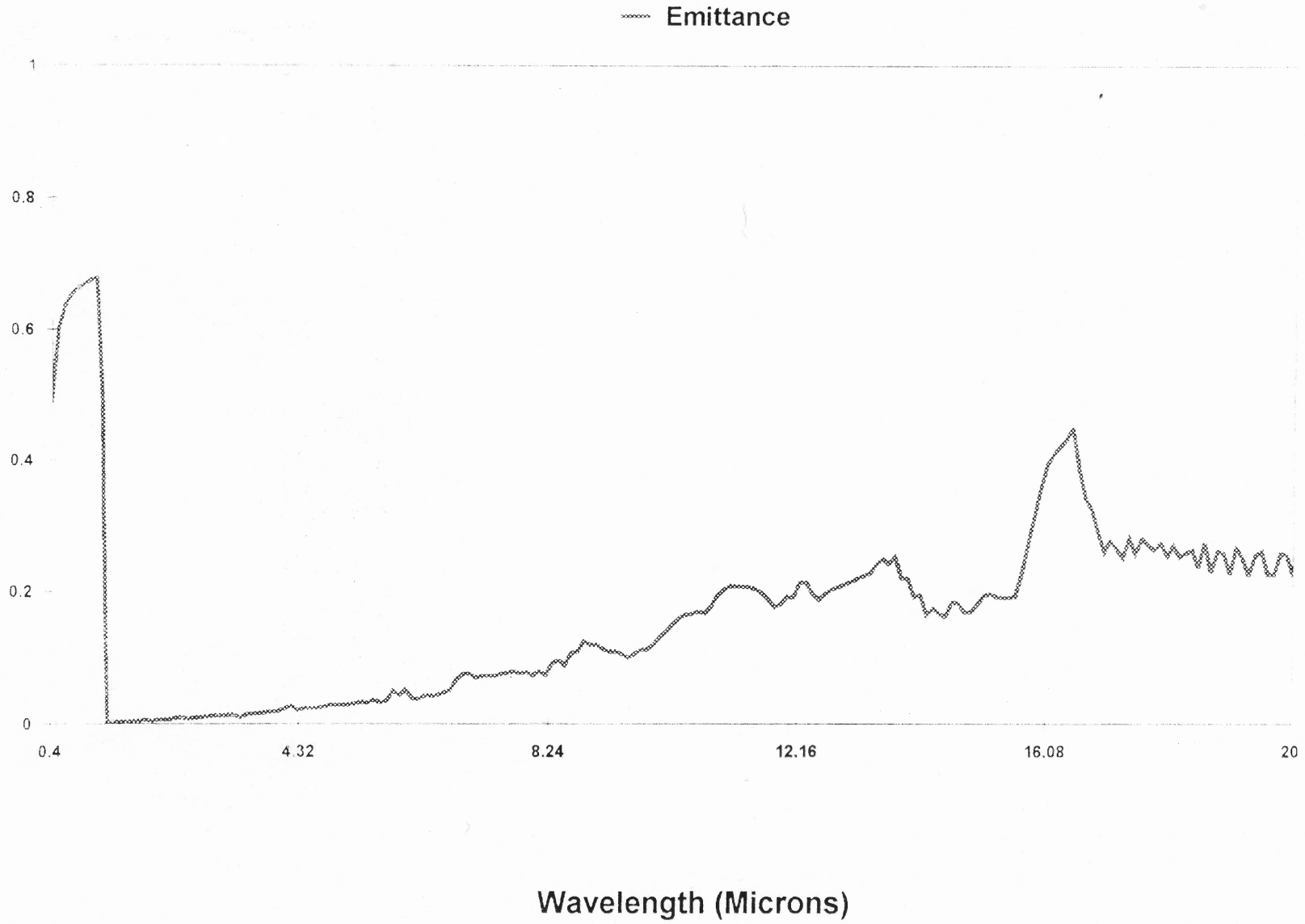

Fig. A2.1 Example of the simulated output of Multi-Rad

APPENDIX III

DATA TABLES

The experimental data of emissivity as a factor of wavenumber, which ranges from 12,500 cm^{-1} to 500 cm^{-1} , for various temperatures are given in this chapter. This chapter includes the experimental data tables for the following samples under investigation (a) Silicon (b) SIMOX (c) Tantalum

- **Silicon**

The experimental data tables for the silicon sample are presented in this section. The variables under consideration are emissivity and wavenumber, at a particular temperature. Tables A3.1, A3.2 and A3.3 illustrate the function of emissivity with respect to wavelength at 30^0 C, 441^0 C and 954^0 C respectively. The experimental data at 263^0 C (cooling) is given in Table A3.4.

- **SIMOX**

The experimental data of the SIMOX sample is presented in Table A3.5. The values of emissivity as a factor of wavenumber, which ranges from 12,500 cm^{-1} (0.8 μm) to 500 cm^{-1} (20 μm) is given in the table.

- **Tantalum**

Table A3.6 gives the experimental data for the tantalum sample. This table illustrates the function of emissivity with respect to wavenumber at room temperature.

Table A3.1 Silicon Sample at RoomTemperature
File DVH

X	Y	X	Y	X	Y	X	Y
12500	-1.50E-01	11758.69	1.70E+01	10044.4	5.00E-01	5472.973	9.88E-01
12484.56	-3.67E-01	11743.24	-5.57E-01	10028.96	5.35E-01	5457.529	9.95E-01
12469.11	########	11727.8	1.54E+01	10013.52	6.63E-01	5442.085	1.00E+00
12453.67	########	11712.36	8.89E-01	9998.07	6.44E-01	5426.641	0.989126
12438.23	8.52E+00	11696.91	1.77E-01	9982.626	7.66E-01	5411.197	9.52E-01
12422.78	6.18E+00	11681.47	-1.96E-01	9967.183	6.88E-01	5395.753	0.965535
12407.34	########	11666.02	3.75E-01	9951.738	5.75E-01	5380.309	9.70E-01
12391.89	1.60E-01	11650.58	5.33E+00	9411.197	7.06E-01	5364.865	9.56E-01
12376.45	4.14E-01	11635.14	1.58E+00	9395.754	7.03E-01	5349.421	0.973742
12361.01	-7.19E-01	11619.69	1.51E+00	9380.31	6.74E-01	5333.977	9.70E-01
12345.56	-8.88E-02	11604.25	2.56E+00	9364.865	7.02E-01	5318.533	9.72E-01
12330.12	########	11588.8	2.56E+00	9349.422	7.41E-01	5303.089	9.77E-01
12314.67	1.37E+00	11573.36	########	9333.978	7.24E-01	5287.645	9.60E-01
12299.23	2.71E+00	11557.92	########	9318.533	6.35E-01	5272.201	9.63E-01
12283.79	########	11542.47	2.13E+00	9303.09	5.90E-01	5256.757	9.67E-01
12268.34	3.00E+00	11527.03	5.54E-01	9287.646	6.42E-01	3897.684	9.80E-01
12252.9	8.65E-01	11511.58	########	9272.201	6.64E-01	3882.24	9.80E-01
12237.45	1.23E+00	11496.14	-0.61996	9256.758	7.01E-01	3866.796	9.79E-01
12222.01	########	10986.49	9.79E-01	9241.314	7.43E-01	3851.352	9.78E-01
12206.56	########	10971.04	1.10E+00	9225.869	7.33E-01	3835.908	9.77E-01
12191.12	########	10955.6	1.09E+00	9210.426	7.45E-01	3820.464	9.78E-01
12175.68	########	10940.16	5.58E-01	9194.981	7.84E-01	3805.02	9.79E-01
12160.23	1.99E+00	10924.71	1.08E+00	9179.537	7.56E-01	3789.575	9.79E-01
12144.79	-4.52E-02	10909.27	1.02E+00	9164.094	7.42E-01	3774.132	9.75E-01
12129.35	########	10893.82	1.16E+00	9148.649	7.37E-01	3758.688	9.71E-01
12113.9	-2.15E-01	10878.38	1.20E+00	8623.553	7.49E-01	3743.243	0.976048
12098.46	3.06E+00	10862.94	5.290361	8608.108	7.50E-01	3727.8	9.80E-01
12083.01	-9.48E-01	10847.49	4.01E+00	8592.665	7.37E-01	3712.356	9.81E-01
12067.57	########	10832.05	1.53E+00	8577.221	7.50E-01	3696.911	9.78E-01
12052.12	########	10816.6	2.26E+00	8561.776	7.60E-01	3681.468	9.78E-01
12036.68	1.39E+00	10801.16	1.52E+00	8546.333	7.58E-01	3666.023	9.79E-01
12021.24	########	10785.72	9.33E-01	8530.889	7.63E-01	747.1043	9.96E-01
12005.79	7.82E+00	10770.27	6.64E-01	8515.444	7.60E-01	731.6603	9.94E-01
11990.35	-2.16E-01	10754.83	7.76E-01	8500.001	7.56E-01	716.2163	9.88E-01
11974.9	-9.00E-02	10739.38	8.47E-01	8484.557	7.54E-01	700.7722	9.86E-01
11959.46	1.45E+00	10723.94	8.65E-01	8469.112	7.64E-01	685.3282	9.78E-01
11944.02	2.02E+00	10708.5	7.67E-01	8453.669	7.66E-01	669.8842	9.73E-01
11928.57	1.30E+00	10198.84	7.68E-01	7835.908	7.78E-01	654.4402	9.84E-01
11913.13	1.82E+00	10183.4	5.71E-01	7820.464	7.70E-01	638.9962	9.88E-01
11897.68	1.03E+00	10167.95	3.04E-01	7805.02	7.52E-01	623.5521	9.89E-01
11882.24	1.51E-01	10152.51	2.92E-01	7789.576	7.54E-01	608.1081	9.88E-01
11866.8	6.80E-01	10137.07	3.78E-01	7774.132	7.58E-01	592.6641	9.94E-01
11851.35	2.26E-01	10121.62	4.15E-01	7758.688	7.66E-01	577.2201	9.89E-01
11835.91	-2.65E-01	10106.18	4.97E-01	7743.244	7.73E-01	561.7761	9.87E-01
11820.46	9.73E-01	10090.73	4.01E-01	7727.8	7.75E-01	546.332	9.82E-01
11805.02	1.38E+00	10075.29	5.33E-01	7712.356	7.64E-01	530.8881	0.968688
11789.58	3.59E+00	10059.85	6.94E-01	7696.912	7.53E-01	500	0.994517

Table A3.2
Silicon at Temperature 441 degrees

X	Y	X	Y	X	Y	X	Y
12500	0.420073	7048.263	0.001686	4932.433	0.004685	1951.738	-0.00064
12484.56	-0.86623	7032.819	0.000234	4916.989	0.007599	1936.294	0.000784
12469.11	-0.01663	7017.375	0.000678	4901.545	0.01285	1920.85	0.000843
12453.67	0.853606	7001.931	-0.00415	4886.101	0.007539	1905.406	0.002029
12438.23	0.318633	6986.487	-0.00388	4870.657	-6.5E-05	1889.962	0.002109
12422.78	0.792593	6971.043	-0.00139	4855.213	0.000822	1874.517	0.000455
12407.34	-0.1332	6955.599	0.001272	4839.769	0.000809	1859.074	-0.00027
12391.89	-0.81795	6940.155	0.001846	4824.325	-0.00037	1148.649	0.000337
12376.45	-0.13031	6924.711	0.002532	4808.881	-0.00467	1133.205	-0.00125
12361.01	-0.65455	6909.267	0.00041	4793.437	0.000577	1117.761	0.000657
12345.56	-0.39496	6893.823	-0.0011	4777.993	0.001524	1102.317	-0.00309
12330.12	-2.78724	6260.618	0.001442	4762.549	-0.002	1086.873	-0.00416
12314.67	-1.63197	6245.174	0.002665	4747.105	-0.00487	1071.429	0.001518
12299.23	-0.54437	6229.73	-0.002	3125.483	0.002043	1055.985	0.000457
12283.79	-0.70505	6214.286	-0.00354	3110.039	0.000546	1040.541	0.002171
12268.34	-0.39967	6198.842	-0.00138	3094.595	0.001496	1025.097	0.003914
12252.9	-0.32143	6183.398	0.003039	3079.151	0.001767	1009.653	0.001528
11789.58	-9.97774	6167.954	0.005889	3063.707	-0.0001	994.2086	0.000217
11774.13	1.106071	6152.51	0.003254	3048.263	-0.00113	978.7645	0.002082
11758.69	-9.74593	6137.066	0.001169	3032.819	-0.00064	963.3205	0.003247
11743.24	0.36301	6121.622	0.00175	3017.375	-0.00017	947.8765	0.001989
11727.8	0.340939	6106.178	0.006193	3001.931	-0.00172	932.4325	0.002358
11712.36	0.473574	6090.734	0.008036	2986.487	-0.00116	916.9885	0.001003
11696.91	-0.47572	6075.29	0.005897	2971.043	0.001876	901.5444	0.000596
11681.47	-0.23751	6059.846	0.004582	2955.599	0.000941	886.1004	-0.00085
11666.02	-0.36389	6044.402	0.002025	2940.155	-0.00042	870.6564	-0.00487
11650.58	0.164885	6028.958	0.001718	2924.711	0.000563	855.2124	-0.00435
11635.14	0.184848	6013.514	0.003114	2909.267	0.00074		
9164.094	0.001013	5998.07	0.002362	2893.823	0.000412		
9148.649	0.009143	5982.626	-0.00046	2878.379	0.000537		
9133.205	-0.00765	5967.182	-0.00499	2862.935	0.000856		
9117.762	0.014344	5951.738	0.00207	2847.491	-0.0001		
9102.317	0.009182	5936.294	0.014327	2832.047	-0.00095		
9086.873	-0.00765	5920.85	0.004958	2816.603	-2.1E-05		
9071.43	-0.02	5905.406	-0.00264	2801.158	0.001402		
9055.985	-0.02785	5117.761	0.00533	2785.714	0.00192		
9040.541	-0.0215	5102.317	-0.00516	2770.271	0.001033		
9025.098	-0.0241	5086.873	0.001671	2106.178	0.000707		
9009.653	0.02062	5071.429	0.007583	2090.734	-0.00021		
8994.209	0.033174	5055.985	0.00044	2075.29	-0.001		
8978.766	0.027697	5040.541	-0.00149	2059.846	-0.00028		
8963.321	0.029991	5025.097	0.001484	2044.402	-3.3E-05		
8947.877	0.016824	5009.653	0.000869	2028.958	-0.0003		
8932.434	0.016689	4994.209	-0.00379	2013.514	-0.00094		
8916.989	0.013042	4978.765	-0.005	1998.07	4.88E-05		
8901.545	0.02127	4963.321	-0.00237	1982.626	0.00155		
8886.101	-0.0024	4947.877	-0.00021	1967.182	0.000107		

Table A3.3
Silicon at 954 degrees - File DWC

X	Y	X	Y	X	Y	X	Y
12500	1.43111	8098.456	0.252455	5025.097	0.251822	2121.622	0.277724
12484.56	-0.03567	8083.012	0.259712	5009.653	0.25693	2106.178	0.276297
12469.11	1.991516	8067.568	0.266294	4994.209	0.258501	2090.734	0.276795
12453.67	0.86448	8052.124	0.264888	4978.765	0.251759	2075.29	0.277083
12438.23	-2.8937	8036.68	0.27311	4963.321	0.258843	2059.846	0.278665
12422.78	-1.89214	8021.236	0.268223	4947.877	0.257755	2044.402	0.279155
12407.34	-0.69607	8005.792	0.269322	4932.433	0.249451	2028.958	0.277413
12391.89	-1.32415	7990.348	0.272829	4916.989	0.248292	2013.514	0.277662
12376.45	0.248373	7974.904	0.271693	4901.545	0.250911	1998.07	0.277163
12361.01	-0.29196	7959.46	0.282096	4886.101	0.253165	1982.626	0.277167
12345.56	-1.55669	7944.016	0.289732	4870.657	0.254138	1967.182	0.276045
12330.12	1.644087	7928.572	0.282752	4855.213	0.262306	1951.738	0.2741
12314.67	-1.61956	7913.128	0.275621	4839.769	0.267599	1936.294	0.274548
12299.23	1.107915	7897.684	0.27101	4824.325	0.267726	1920.85	0.274828
12283.79	0.839955	7882.24	0.280722	4808.881	0.263958	1905.406	0.275546
12268.34	0.918768	7866.796	0.281508	4793.437	0.258479	1889.962	0.276731
12252.9	0.973358	7851.352	0.266463	4777.993	0.259601	1874.517	0.277345
10198.84	0.13668	7835.908	0.260783	4762.549	0.263428	1859.074	0.275155
10183.4	0.132199	7820.464	0.26802	4747.105	0.267107	1843.629	0.273995
10167.95	0.136014	7805.02	0.283636	4731.661	0.266391	1828.185	0.275021
10152.51	0.046102	7789.576	0.289645	4716.217	0.26495	1812.741	0.276169
10137.07	0.057923	7774.132	0.28837	4700.773	0.267361	1797.297	0.276122
10121.62	0.020012	7758.688	0.286982	4685.329	0.266956	1781.853	0.277915
10106.18	-0.00995	7743.244	0.288904	4669.884	0.264461	1766.409	0.280178
10090.73	0.072886	7727.8	0.289052	3187.259	0.27983	839.7684	0.302775
10075.29	0.242093	6167.954	0.29924	3171.815	0.276076	824.3243	0.299109
10059.85	0.285846	6152.51	0.300998	3156.371	0.276591	808.8803	0.297095
10044.4	0.190406	6137.066	0.299101	3140.927	0.277877	793.4363	0.293963
10028.96	0.200935	6121.622	0.295004	3125.483	0.278908	777.9923	0.291699
10013.52	0.311928	6106.178	0.2933	3110.039	0.280635	762.5483	0.289052
9998.07	0.379405	6090.734	0.297955	3094.595	0.281314	747.1043	0.280065
9982.626	0.305861	6075.29	0.297274	3079.151	0.2809	731.6603	0.278375
9967.183	0.245749	6059.846	0.298073	3063.707	0.279862	716.2163	0.279317
9951.738	0.369342	6044.402	0.300629	3048.263	0.281092	700.7722	0.27315
9936.294	0.25272	6028.958	0.29247	3032.819	0.280923	685.3282	0.267204
9920.851	-0.04775	6013.514	0.296276	3017.375	0.27889	669.8842	0.27339
9905.406	-0.12453	5998.07	0.310327	3001.931	0.281007	654.4402	0.279826
9889.962	-0.01743	5982.626	0.31469	2986.487	0.282254	638.9962	0.28166
9133.205	0.233558	5967.182	0.304769	2971.043	0.283541	623.5521	0.28278
9117.762	0.277246	5951.738	0.296128	2955.599	0.283969	608.1081	0.286834
9102.317	0.242391	5936.294	0.290753	2940.155	0.282193	592.6641	0.291165
9086.873	0.224803	5920.85	0.277548	2924.711	0.283168	577.2201	0.278431
9071.43	0.194837	5905.406	0.264564	2909.267	0.28331	561.7761	0.281469
9055.985	0.17642	5889.962	0.279462	2893.823	0.281329	546.332	0.308304
9040.541	0.201676	5874.518	0.290224	2878.379	0.282335	530.8881	0.314044
9025.098	0.245323	5859.074	0.279542	2862.935	0.282865	515.444	0.321189
9009.653	0.249277	5843.63	0.278257	2847.491	0.281905	500	0.316834

Table A3.4
Silicon at 263 degrees (cooling) –
FileDWE

X	Y	X	Y	X	Y	X	Y
12500	-5.33142	9472.974	0.227994	7310.812	0.251059	1256.757	0.206846
12484.56	-3.33964	9457.529	0.1339	7295.367	0.252642	1241.313	0.209516
12469.11	1.502267	9442.086	0.081077	7279.923	0.262143	1225.869	0.20919
12453.67	3.530786	9426.642	0.17598	7264.48	0.26306	1210.425	0.20638
12438.23	1.806723	9411.197	0.194477	7249.035	0.254515	1194.981	0.212232
12422.78	0.707137	9395.754	0.172862	7233.591	0.261954	1179.537	0.213406
12407.34	1.35892	9380.31	0.168062	7218.148	0.261009	1164.093	0.212845
12391.89	2.080568	9364.865	0.245763	7202.703	0.278423	1148.649	0.209376
12376.45	0.07011	9349.422	0.253718	7187.259	0.289271	1133.205	0.203543
12361.01	-1.30428	9333.978	0.246516	7171.815	0.274017	1117.761	0.212585
12345.56	-1.42824	9318.533	0.10632	7156.371	0.270209	1102.317	0.222472
12330.12	-7.76257	9303.09	0.116441	7140.927	0.28229	1086.873	0.221355
12314.67	-9.00502	9287.646	0.252118	7125.483	0.278307	1071.429	0.220324
12299.23	1.100276	9272.201	0.270386	7110.039	0.260871	1055.985	0.216984
12283.79	1.532522	9256.758	0.273392	7094.595	0.271906	1040.541	0.209343
12268.34	1.055007	9241.314	0.18442	7079.151	0.278124	1025.097	0.211707
12252.9	0.251333	9225.869	0.114036	7063.707	0.276903	1009.653	0.217848
12237.45	0.871955	9210.426	0.14351	7048.263	0.261453	994.2086	0.218796
12222.01	3.612421	9194.981	0.223901	7032.819	0.248706	978.7645	0.216055
12206.56	5.017348	9179.537	0.250267	7017.375	0.261755	963.3205	0.21634
12191.12	9.197743	9164.094	0.27942	7001.931	0.273926	947.8765	0.215314
12175.68	16.47105	9148.649	0.230667	6986.487	0.276758	932.4325	0.211993
12160.23	-16.583	9133.205	0.190697	6971.043	0.277234	916.9885	0.208632
12144.79	-6.35891	9117.762	0.192126	6955.599	0.284723	901.5444	0.20162
12129.35	75.14258	9102.317	0.148857	6940.155	0.283269	886.1004	0.207171
12113.9	67.98288	9086.873	0.074464	6924.711	0.277252	870.6564	0.217335
12098.46	14.42172	9071.43	0.080995	6909.267	0.278933	855.2124	0.223179
12083.01	5.5505	9055.985	0.182338	6893.823	0.272297	839.7684	0.220181
12067.57	0.219607	9040.541	0.183569	6878.379	0.27206	824.3243	0.210501
12052.12	39.54146	9025.098	0.192699	6862.935	0.277131	808.8803	0.208905
12036.68	2.449712	9009.653	0.153153	6847.491	0.280723	793.4363	0.20676
12021.24	0.704527	8994.209	0.169525	6832.047	0.278034	777.9923	0.197679
12005.79	-1.69387	8978.766	0.135929	6816.603	0.274453	762.5483	0.18696
11990.35	-1.99336	8963.321	0.098757	6801.159	0.271949	747.1043	0.180446
11974.9	-2.07715	8947.877	0.233214	6785.715	0.266441	731.6603	0.183727
11959.46	0.878731	8932.434	0.252273	6770.271	0.265033	716.2163	0.188069
11944.02	0.824733	8916.989	0.292091	6754.827	0.268919	700.7722	0.18404
11928.57	0.832984	8901.545	0.347735	6739.383	0.273171	685.3282	0.182479
11913.13	1.132279	8886.101	0.270843	6723.939	0.274791	669.8842	0.175414
11897.68	-18.0304	8870.657	0.247448	6708.495	0.270159	654.4402	0.163591
11882.24	9.111146	8855.213	0.227082	6693.051	0.270252	638.9962	0.154642
11866.8	0.782046	8839.769	0.232944	6677.606	0.268516	577.2201	0.1251
11851.35	-8.77184	8824.325	0.289679	6662.163	0.266886	561.7761	0.114179
11835.91	2.290969	8808.881	0.249457	6646.719	0.269528	546.332	0.105802
11820.46	0.967904	8793.437	0.247606	6631.274	0.270902	530.8881	0.055394
11805.02	-5.24866	8777.993	0.263813	6615.831	0.270097	515.444	0.014389

Table A3.5 - SIMOX at Room Temperature - File DXD

X	Y	X	Y	X	Y			
12500	-0.73474	10245.18	-0.94298	7928.572	-0.33441	5225.869	-1.56567
12484.56	0.171546	10229.73	0.223681	7913.128	-0.33247	5210.425	-1.58014
12469.11	0.298019	10214.29	0.704055	7897.684	-0.36325	5194.981	-0.62315
12453.67	0.158616	10198.84	0.924749	7882.24	-0.32152	5179.537	-0.60982
12438.23	0.08102	10183.4	1.464323	7866.796	-0.24983	5164.093	-1.22254
12422.78	-0.39842	10167.95	1.20548	7851.352	-0.29162	5148.649	-1.40214
12407.34	-2.46772	10152.51	-2.43434	7835.908	-0.32027	5133.205	-1.31656
12391.89	23.09115	10137.07	-3.14372	7820.464	-0.29761	5117.761	-0.67005
12376.45	7.48527	10121.62	0.09304	7805.02	-0.31487	5102.317	-0.10076
12361.01	11.75665	10106.18	0.369808	7789.576	-0.30895	5086.873	0.21695
12345.56	1.539797	10090.73	0.841822	7774.132	-0.32709	5071.429	0.191706
12330.12	2.47625	10075.29	0.174034	7758.688	-0.30957	5055.985	-0.69438
12314.67	15.52556	10059.85	-0.10105	7743.244	-0.30433	5040.541	-0.75761
12299.23	-1.06773	10044.4	-1.18741	7727.8	-0.34432	5025.097	-0.72918
12283.79	0.13404	10028.96	-2.27297	7712.356	-0.31945	5009.653	-0.31815
12268.34	-4.32092	10013.52	-0.50498	7696.912	-0.28146	4994.209	0.062649
12252.9	-0.31006	9998.07	-0.63344	7681.468	-0.253	4978.765	-0.26373
12237.45	-1.30496	9982.626	-0.69865	7666.024	-0.28414	4963.321	-0.44858
12222.01	4.356339	9967.183	-0.62004	7650.58	-0.32984	4947.877	-0.96148
12206.56	-205.889	9951.738	0.543218	7635.136	-0.34387	4932.433	-0.93967
12191.12	0.350793	9936.294	0.000114	7619.692	-0.36329	947.8765	-0.32496
10986.49	9.348659	9920.851	-0.6	6384.17	-0.35134	932.4325	-0.34644
10971.04	3.986503	9905.406	-0.41323	6368.727	-0.35045	916.9885	-0.31489
10955.6	0.697331	8700.773	-0.37296	6353.282	-0.31742	901.5444	-0.34259
10940.16	3.321044	8685.329	-0.42147	6337.838	-0.30146	886.1004	-0.37736
10924.71	0.110655	8669.885	-0.36866	6322.395	-0.30445	870.6564	-0.31362
10909.27	-0.6129	8654.44	-0.35766	6306.95	-0.32366	855.2124	-0.26946
10893.82	-2.39684	8638.997	-0.38512	6291.506	-0.32773	839.7684	-0.3052
10878.38	-1.89271	8623.553	-0.26627	6276.062	-0.35616	824.3243	-0.29836
10862.94	-7.96937	8608.108	-0.2531	6260.618	-0.39713	808.8803	-0.31362
10847.49	-3.70035	8592.665	-0.4355	6245.174	-0.37788	762.5483	-0.34076
10832.05	-0.41684	8577.221	-0.49652	6229.73	-0.36407	747.1043	-0.40048
10816.6	-0.77889	8561.776	-0.34076	6214.286	-0.37009	731.6603	-0.35756
10801.16	-2.1244	8546.333	-0.37191	6198.842	-0.35337	716.2163	-0.32255
10785.72	1.808123	8530.889	-0.41184	6183.398	-0.3446	700.7722	-0.26027
10770.27	1.736467	8515.444	-0.30483	6167.954	-0.34474	638.9962	0.096531
10754.83	2.33052	8500.001	-0.36346	6152.51	-0.32856	623.5521	-0.22702
10739.38	-2.43257	8484.557	-0.35525	6137.066	-0.33988	608.1081	-0.66568
10723.94	-1.33315	8469.112	-0.27675	6121.622	-0.3417	592.6641	-0.18603
10708.5	34.85929	8453.669	-0.26059	6106.178	-0.32754	577.2201	0.238413
10693.05	0.138318	8438.225	-0.31828	6090.734	-0.34939	561.7761	-0.04216
10677.61	-0.16581	8422.78	-0.38422	6075.29	-0.28599	546.332	-0.54031
10662.16	-0.43258	8407.337	-0.31479	6059.846	-0.28255	530.8881	-1.11454
10646.72	-1.29982	8391.893	-0.25454	6044.402	-0.32735	515.444	-0.02464
10631.28	-0.35697	8376.448	-0.24563	6028.958	-0.36658	500	3.892637

Table A3.6
Tantalum Sample at Room Temperature - File DWT

X	Y	X	Y	X	Y	X	Y
12500	22.56941	10971.04	0.413154	8546.333	-0.23629	5534.75	-0.0158
12484.56	-4.44461	10955.6	0.536208	8530.889	-0.15956	5519.306	-0.03018
12469.11	-0.36553	10940.16	1.672814	8515.444	-0.13043	5503.861	-0.00733
12453.67	1.612829	10924.71	0.118175	8500.001	-0.18025	5488.418	0.02015
12438.23	0.627787	10909.27	-0.01082	8484.557	-0.22389	5472.973	0.024928
12422.78	2.153234	10893.82	0.131018	8469.112	-0.18214	4669.884	0.000864
12407.34	13.58321	10878.38	-1.07935	8453.669	-0.16141	4654.44	-0.00287
12391.89	46.05808	10862.94	-2.18993	8438.225	-0.19284	4638.997	-0.01028
12376.45	-1.95187	10847.49	0.563135	8422.78	-0.17316	4623.552	-0.03141
12361.01	-3.36604	10832.05	1.542176	8407.337	-0.17388	4608.108	-0.0136
12345.56	-2.7424	10816.6	-0.51007	8391.893	-0.17017	4592.665	-0.00487
12330.12	-41.6607	10801.16	-2.09105	8376.448	-0.14041	4577.22	-0.00032
12314.67	-13.9896	10785.72	-0.47169	8361.005	-0.16461	4561.776	-0.00064
12299.23	2.0304	10770.27	-0.9687	8345.561	-0.17816	4546.333	-0.00097
12283.79	7.325157	10754.83	-0.83985	7032.819	-0.18486	4530.888	-0.01132
12268.34	-14.6743	10739.38	0.385965	7017.375	-0.17866	4515.444	-0.01639
12252.9	-9.35259	10723.94	3.53606	7001.931	-0.18208	4500.001	-0.01711
12237.45	11.83424	10183.4	-0.79734	6986.487	-0.18974	4484.556	-0.02173
12222.01	5.099723	10167.95	-0.4528	6971.043	-0.18352	4469.112	0.000271
12206.56	7.007972	10152.51	-0.49494	6955.599	-0.17218	4453.668	0.003403
12191.12	0.75981	10137.07	-0.27766	6940.155	-0.17208	4438.224	-0.00756
12175.68	0.068158	10121.62	0.083633	6924.711	-0.17325	793.4363	0.003689
11758.69	-0.6398	10106.18	-0.1003	6909.267	-0.16149	777.9923	0.00271
11743.24	-0.39374	10090.73	-0.38339	6893.823	-0.16168	762.5483	-0.00236
11727.8	-0.35283	10075.29	-0.22296	6878.379	-0.17767	747.1043	0.00627
11712.36	0.543415	10059.85	-0.14646	6862.935	-0.17777	731.6603	0.016501
11696.91	1.915014	10044.4	0.009453	6847.491	-0.17695	716.2163	0.013937
11681.47	5.392994	10028.96	0.061304	6832.047	-0.17887	700.7722	-0.02306
11666.02	-0.78618	10013.52	-0.15329	6816.603	-0.17273	685.3282	0.006523
11650.58	-0.76523	9998.07	-0.07678	6801.159	-0.17797	669.8842	0.009987
11635.14	0.293493	9982.626	-0.16034	6785.715	-0.18212	654.4402	0.003677
11619.69	0.659526	9967.183	-0.25984	6770.271	-0.17683	638.9962	-0.00657
11604.25	0.218771	9951.738	-0.0412	6754.827	-0.17741	623.5521	-0.00475
11588.8	0.79588	9936.294	0.195798	6739.383	-0.17564	608.1081	-0.07845
11573.36	0.41625	9395.754	-0.09365	6723.939	-0.17556	592.6641	-0.02455
11557.92	-0.39919	9380.31	-0.15521	5735.522	-0.03151	577.2201	-0.02239
11542.47	-0.24592	9364.865	-0.19949	5720.078	0.01215	561.7761	0.01994
11527.03	0.476853	9349.422	-0.15564	5704.634	-0.02283	546.332	-0.08546
11511.58	-12.5916	9333.978	-0.06428	5689.189	-0.07451	530.8881	0.058897
11496.14	-2.35052	9318.533	-0.04351	5673.746	-0.06509	515.444	-0.00487
11480.7	-7.3649	9303.09	-0.22886	5658.302	-0.05898	500	0.003624
11465.25	-1.43438	9287.646	-0.25313	5642.857	-0.05271		
11449.81	-0.07559	9272.201	-0.13757	5627.414	-0.03525		
11434.36	0.13669	9256.758	-0.17547	5611.97	-0.03102		
11418.92	-0.3432	8608.108	-0.16293	5596.525	-0.02129		
11403.48	1.450154	8592.665	-0.16929	5581.082	-0.02489		
11388.03	55.26544	8577.221	-0.10401	5565.638	-0.02165		

11372.59 -0.30477 8561.776 -0.15538 5550.193 -0.00955

Note : In the wavenumber range of 12,500 cm^{-1} to 10,000 cm^{-1} , the signal to noise ratio is very poor. Therefore, the detector limit of the emissometer is not reliable. Obviously, any existence of negative integers need to be neglected completely.

APPENDIX IV

DOPING

The effect of doping is discussed in this chapter. The Multi-Rad model supports doping type in determining the value of emissivity as a function of wavelength. The variations in the carrier concentrations are based on the resistivity, which is supported by Multi-Rad.

- P-type

The normalized mathematical equation for the value of carrier concentration, at room temperature, is given below.

$N = 1/ q\rho \{ K_{min} + [K_{max} - K_{min} / (1 + \rho / \rho_{ref})^{\alpha}] \}$

where 'q' is the charge, 'ρ' is the resistivity, 'N' is the carrier concentration.

$K_{min} = 2.13 \times 10^{-3}$; $K_{max} = 1.947 \times 10^{-2}$; $\rho_{ref} = 1.833 \times 10^{-2}$; $\alpha = 1.105$

Using the above equation, values of carrier concentration can be computed for change in values of resistivity. The table below illustrates the change in carrier concentration for values of resistivity ranging from 100 Ω - cm to 0.1 Ω - cm

Resistivity	N
100	1.33×10^{14}
10	1.33×10^{15}
1	1.46×10^{16}
0.1	2.77×10^{17}

- N type

The normalized mathematical equation for the value of carrier concentration, at room temperature, is given below.

$N = \{ / q\rho \} * 10^{A_1} w$

where A1 is a normalized polynomial, which is as follows,

$A_1 = (a_0 + a_1 x + a_2 x^2 + a_3 x^3) / (1 + b_0 + b_1 x + b_2 x^2 + b_3 x^3)$

where 'q' is the charge ; 'ρ' is the value of resistivity ; $x = \log_{10}(\rho)$

$a_0 = -3.1 \pm 0.003$; $a_1 = -3.26 \pm 0.09$; $a_2 = -1.21 \pm 0.03$; $a_3 = -0.13 \pm 0.004$

$b_1 = 1.02 \pm 0.03$; $b_2 = 0.38 \pm 0.01$; $b_3 = 0.04 \pm .0.01$

REFERENCES

1. F.Roozeboom, *Advances in Rapid Thermal and Integrated Processing*, Vol.318, p.35-51, Kluwer Academic Publishers, Boston, MA, July, (1995).

2. S.Wolf and R.N. Tuber, *Silicon Processing for VLSI Era*, Vol.1, Lattice Press, CA , (1986).

3. G.L. Miller, *Tantalum and Niobium*, Butterworth Scientific Publications, London, (1942).

4. R.M.Burger and R.P. Donovan, *Fundamentals of Silicon Integrated Device Technology*, Vol.II, Prentice- Hall Inc., NJ, (1968).

5. Ben G. Streetman, *Solid State Electronic Devices*, Prentice Hall Inc., NJ, (1990).

6. Quick Reference Manual, *Silicon Integrated Circuit Technology*, John Wiley & Sons., NY, (1985).

7. S.Abedrabbo, J.C. Hensel, A.T.Fiory, B.Sopori, W.Chen, N.M.Ravindra, "Perspectives on Emissivity measurements and modelling in silicon" Proc. of MRS Symposium, Vol.2, p.95-102, (1998).

8. J.R. Markham, *A Bench Top FT-IR Based Instrument for Simultaneous Measuring Surface Spectral Emittance and Temperature, Review Scientific Instruments*, Vol.64, No.9, p.2515-2522, (1993).

9. W.L. Wolfe and G.J.Zissis, *Infrared Handbook* , Environmental Research Institute Michigan, Ann Arbor, MI, (1989).

10. M.Bass, *Handbook of Optics - Device Measurements, and Properties*, 2nd edition, Vol.2, Chapman & Hall, London, (1994).

11. K.Sato, "Spectral emissivity of silicon", Japanese Journal of App.Phys., Vol.6, no.3, p. 339- 347, (1967).

12. N.M Ravindra, S.Abedrabbo, W.Chen, F.M.Tong, A.Nanda and A. Speranza, " Temperature-Dependent Emissivity of Silicon-Related Materials and Structures", IEEE transactions on Semiconductor Manufactring, Vol.11, no.1, p.30-38, (1998).

13. William R. Wade, " Measurements of Total Hemispherical Emissivity of various oxidized metals at high temperature", Technical note 4206, National Advisory Committee for Aeronautics, p. 1-11, Washington, (1958).

14. N. M. Ravindra, S. Abedrabbo, O.H. Gokce, Feiming Tong, A. Patel, R. Velagapudi, G. D. Williamson and W.P. Maszara, " Radiative Properties of SIMOX ", IEEE Transactions on Components, Packaging and Manufacturing Technology – Part A, Vol.21, no.3, p. 441-448, (1998).